

OPEN ACCESS

EDITED BY

Biswajeet Pradhan, University of Technology Sydney, Australia

REVIEWED BY

Bibhuti Bhusan Sahoo, Centurion University of Technology and Management School of Engineering and Technology, India Devrajsinh Thakor, Indian Council of Agricultural Research-Indian Veterinary Research Institute, India

*CORRESPONDENCE Pankaj Kumar,

□ pankajdsedu@gmail.com
 RECEIVED 08 August 2025

REVISED 14 October 2025 ACCEPTED 23 October 2025 PUBLISHED 11 November 2025

CITATION

Sarda R and Kumar P (2025) Monitoring the dual-season hydrological dynamics of the Pong reservoir in Himachal Pradesh, India. *Front. Remote Sens.* 6:1682140. doi: 10.3389/frsen.2025.1682140

© 2025 Sarda and Kumar. This is an open-

access article distributed under the terms of the Creative Commons Attribution License (CC BY). The use, distribution or reproduction in other forums is permitted, provided the original author(s) and the copyright owner(s) are credited and that the original publication in this journal is cited, in accordance with accepted academic practice. No use, distribution or reproduction is permitted which does not comply with these terms.

Monitoring the dual-season hydrological dynamics of the Pong reservoir in Himachal Pradesh, India

Rajesh Sarda and Pankaj Kumar*

Department of Geography, Delhi School of Economics, University of Delhi, New Delhi, India

Reservoir hydrological conditions play a crucial role in both natural and human ecosystems. This study investigates the dual-season (pre-monsoon and postmonsoon) hydrological dynamics of the Pong Reservoir and analyzing the spatial character using Landsat multi-spectral images collected from 1994 to 2024. The 30 years were divided into three phases to assess changes in hydrological consistency and relative water depth over time. The Modified Normalized Difference Water Index (MNDWI) proved effective for mapping the water coverage area of the Pong Reservoir. Analysis based on MNDWI indices reveals significant seasonal fluctuations in water coverage, with 36.18 km² of the reservoir exhibiting seasonal characteristics. Furthermore, the phase-wise results indicate a substantial decline in the area of high hydrological consistency during the pre-monsoon season, from 120.54 km² in Phase 1 (1994-2004) to 88.49 km² in Phase 3 (2015–2024). The change matrix indicates that 10.62 km² transformed from higher to lower hydrological consistency classes from Phase 1 to Phase 2, and a further 51.97 km² underwent a similar transformation from Phase 2 to Phase 3 in the post-monsoon season. The study employed a spatial linear trend modelling approach to identify trends in relative water depth, revealing a decreasing trend and a quantifiable reduction in the reservoir's depth for both seasons. Additionally, further analysis was conducted on the impact of seasonal rainfall and sedimentation on the hydrological dynamics of the Pong Reservoir. These findings could assist policymakers in formulating effective conservation plans for this important Ramsar site.

KEYWORDS

reservoir, spatio-temporal analysis, hydrological consistency, relative water depth, linear trend modelling

1 Introduction

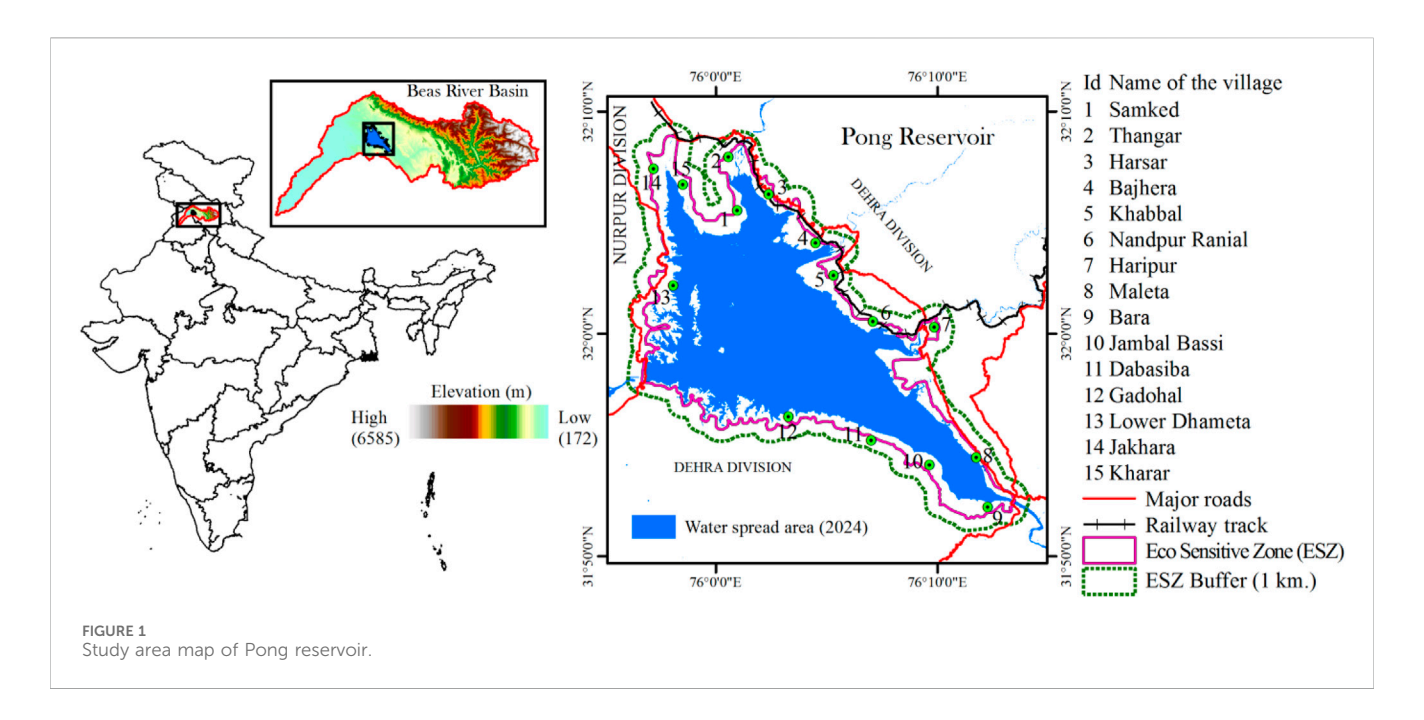
Anthropogenic function is responsible for maximum modifications of the fluvial landscape features on the regional to global scale, one of which is the construction of dams over rivers (Ekka et al., 2020). The construction of reservoirs to capture surface water is a common practice across the globe (Donchyts et al., 2022). The river damming conception is largely done by prioritising the positive appearance of human wellbeing, viz., socio-economic development, hydro-ecological importance, and environmental advantages. It provides expensive services such as water supply for irrigation, hydroelectric power generation, flood protection, transportation, and recreational activities (Guo et al., 2021; Zhao et al., 2022; Mácová and Kozáková, 2023). On the other side, it significantly affects the downstream rivers hydrological regime, particularly

through changes in the magnitude, timing, and recurrence of flows (Haghighi et al., 2014). So, the construction of reservoirs over rivers has both some benefits and burdens (Połomski and Wiatkowski, 2023). Without much extending the benefits burden debate, this discussion focuses solely on the positive aspects of human-made reservoirs, which face some emerging threats (Ho and Goethals, 2019). The excessive water demand due to increasing population, sedimentation, climate change, the inherent variability of precipitation, and river discharge were the major threats to the hydrological character of the reservoir (Ghosh and Chakraborty, 2021; Krztoń et al., 2022; Patro et al., 2022; Verma et al., 2023). All the mentioned threats have reached such an extent that they jeopardize the reliability of reservoir hydrological functions (Ayele et al., 2021).

The hydrological regime of the man-made reservoirs differs significantly from that of natural wetlands, such as rivers and lakes (Sarda and Pal, 2024). The natural wetland strongly depends on rainfall and river inundation for water recharge. However, their outlet systems are often inadequate, resulting in a prolonged period of standing water. In contrast, man-made wetlands typically have more effective outlet systems. While they receive water from natural sources, the discharge from reservoirs is closely regulated by the concerned authorities. Thus, it creates a highly controlled water management system. This regulation leads to distinct hydrological characteristics, including the frequency and magnitude of water level fluctuations, as well as the timing and duration of these changes are quite distinct from those of natural wetlands. These unique characteristics have a substantial impact on the health of the wetland ecosystem. For example, the shallow water depths and limited surface areas make the reservoirs ecologically fragile and less resilient in terms of the aquatic ecosystem. Therefore, a thorough understanding of the hydrological characteristics of a reservoir is not merely a technical exercise but a crucial prerequisite for developing sustainable management strategies and ensuring long-term viability its vital environmental resource.

Recent advancements in remote sensing technology have significantly improved the mapping and monitoring of surface water dynamics (Cazenave et al., 2016). This technology offers more accurate and reliable information than conventional in-situ measurements due to its ability to monitor the Earth at various spatial and temporal scales continuously (Sogno et al., 2022). The integration of remote sensing data in water resource applications can effectively aid in formulating sustainable management plans. Over time, various approaches have been introduced to delineate water cover areas. Among them, the spectral water indices approach is well-recognised and easy to use for real-time monitoring of surface water across the globe. Various spectral water index techniques have been developed to delineate water bodies from multi-spectral satellite imagery. Supplementary Table S1 provides a comprehensive overview of different spectral water indices used for mapping surface water cover. These techniques are continually updated and widely used. Based on the literature survey, it can be concluded that the Normalized Difference Water Index (NDWI) is most suitable for delineating open water bodies (McFeeters, 1996). The NDWI, which was designed to extract water features using the green and near-infrared (NIR) bands of the Landsat Thematic Mapper (TM), with a threshold of zero, has been found ineffective in correctly distinguishing built areas from water surfaces (McFeeters, 1996). In addition to open water bodies, the Modified NDWI (MNDWI) is often suitable for identifying wetlands with wet soil, as well as for clearly depicting reservoir water cover, urban lakes, and river channels. Xu (2006) modified the MNDWI by replacing the NIR band with the middle infrared band of Landsat-5 Thematic Mapper. This modification enhances the contrast between water and non-water features, helping to eliminate signals from built-up areas and dark soils. Recently, the Re-Modified NDWI (RmNDWI) has been successfully applied for wetland mapping (Debanshi and Pal, 2020). Debanshi and Pal (2020) introduced the RmNDWI by using information from the red band instead of the green band. However, not all the water extraction indices are equally applicable across the globe, while the performance of those water extraction indices will vary in different situations (Zhai et al., 2015). Considering this space's respective applicability of the water extraction indices, the present work has attempted to use a multi-index approach and selected the best suitable index via a validation process.

Many researchers have investigated reservoir hydrological dynamics focusing on issues like climate change, sedimentation, and anthropogenic pressure (Amasi et al., 2021; Matlhodi et al., 2021; Kahaduwa and Rajapakse, 2022). Most of the studies primarily focused on the changes in water cover area by using a single-date satellite image, but studies on water cover consistency (dual-season) using multi-date satellite images have not been done yet. Reservoir hydrological consistency in water cover can indicate which part possesses consistent water presence and which areas store water inconsistently or no longer retain it. The water presence frequency approach could be a good measure to examine the reservoir hydrological consistent character (Sarda and Das, 2018; Taheri Dehkordi et al., 2022). It can easily figure out consistent/ inconsistent water-retaining reservoir areas at a spatial scale. Therefore, this research will provide valuable references in proposing a sustainable management plan for the reservoir. On the other side, Water depth is another crucial hydrological component, which is directly linked to the species diversity, richness, and comfort (Asher et al., 2017; Yang et al., 2020). However, infrastructures for continuous monitoring of reservoir depth are not always available in all reservoirs. In these circumstances, multi-temporal satellite images can be an effective approach for monitoring the reservoir depth. Most of the studies found the linear relationship between the spectral water index value and depth of surface water (Talukdar and Pal, 2019; Pal and Sarda, 2021; Khatun et al., 2021). So, this study considered the water indices value as the relative depth of the reservoir and examined the spatial hydrological performance over time. Spatial trends in reservoir water depth need to be assessed for any sustainable management planning (Daus et al., 2021). Many researchers investigate historical trends (pixel-wise) for surface water, crop health, and other environmental components using a linear regression modelling approach (Debanshi and Pal, 2020; Pal and Paul, 2021; Pal et al., 2022). Although no studies have been carried out on utilizing a linear trend modelling approach to examine the pixel-wise changes in the hydrological character of the reservoir. Therefore, in this research, we developed a pixel-wise trend map that represents the reservoir hydrological character. The analysis was done by applying a linear regression model, taking into account long-term time series



water indices maps spanning 30 years. As a result, the outcome provides very detailed insights about the changes in the reservoir's hydrological conditions.

This work is very instrumental and could be helpful to the management authorities for formulating any management plans at a very fine scale. So, the essential objectives of this study are summarised as (i) To extract water bodies using different water extraction indices along with validation techniques and select a suitable water index for further analysis; (ii) Monitoring dual season spatio-temporal differences of hydrological consistent areas for 3 decades (1994–2024); and (iii) Recognize the seasonal dynamics of reservoir relative water depth using spatial linear trend modelling approach from 1994 to 2024.

2 Study area

Pong Reservoir, located in the Kangra district of Himachal Pradesh, was constructed as an earthen management dam. It is also known as the Maharana Pratap Sagar Reservoir. The Beas River and its tributaries predominantly influence the hydrological dynamics of the reservoir. It is the largest man-made wetland in Northern India, which intercepts the Trans-Himalayan flyway. This man-made wetland was listed as a site of national importance in 1994 and incorporated as a Ramsar site in 2002 based on the immense diversity of waterfowl it supports. Thus, the Union Ministry of Environment and Forests has recently issued a draft notification (on 28 April 2022) declaring an area of 1 km from the boundaries of Pong Dam Wildlife Sanctuary as an Eco-Sensitive Zone (ESZ) (Figure 1). The total coverage area of pong reservoir is 245.29 km² including 156.62 km² notified as a Ramsar wetland area. The catchment area of the Pong Reservoir covers approximately 12,561 km² and has a storage capacity of about 7,290,000,000 m³. This reservoir is situated in a subtropical monsoon climate, where maximum rainfall occurs during the monsoon months from June to September. The monsoon rainfall contributes around 57% of the total annual rainfall, while the post-monsoon period from October to December accounts for about 18% of the total rainfall. The remaining seasons experience low rainfall and high rates of evapotranspiration. As a result, water availability and the surface area of the reservoir are maximum during the monsoon period. For this research, we created a spatial buffer with a radius of 1 km around the Eco-Sensitive Zone (ESZ) of the Pong Reservoir.

3 Materials

Landsat satellite images are valuable remote sensing datasets, which are widely used for monitoring landscape features over time. Many researchers used this dataset because of its free availability. In this research work, a total of 170 multi-temporal Landsat satellite images (Level-2) for the pre- and post-monsoon seasons were collected from 1994 to 2024. These satellite images were downloaded from the United States Geological Survey (USGS) Earth Explorer website (Table 1). The details of the sensors and image acquisition dates were mentioned in the supplementary section (Supplementary Table S2). The reservoir area was initially delineated using Google Earth images; however, raw satellite imagery was not useful for extracting information. To enhance its usefulness, the other necessary corrections were made using geospatial software.

4 Methods

4.1 Method for reservoir water cover area mapping

Many spectral indices have been utilized to identify different landscape features like water body, vegetation, built-up area etc. In this connection, various spectral water indices were developed for mapping water cover area like Normalized Difference Water Index

Key information	Landsat-5	Landsat-7	Landsat-8	Landsat-9			
Sensor	TM	ETM	OLI-TIRS				
Period of acquisition year	1994–2011	2000-2013	2014-2024	2022-2024			
Total number of images	52	58	48	12			
Path/row	148/38						
Spatial resolution (m)	30 m						
Note		Cloud Cover less than 10%					

TABLE 1 Information about the satellite imagery used in this study.

(NDWI) (Mcfeeters, 1996), General Water Index (GWI) (Yang and Xu, 1998), Modified Normalized Difference Water Index (MNDWI) (Xu, 2006), Water Ratio Index (WRI) (Shen and Li, 2010), New Water Index (NWI) (Feng, 2009), Automated Water Extraction Index (AWEI) (Feyisa et al., 2014), Re-modified Normalized Difference Water Index (RmNDWI) (Debanshi and Pal, 2020) etc. However, the effectiveness of these water indices varies across different regions. In this research work, three spectral water indices (NDWI, MNDWI and RmNDWI) were utilized to delineate reservoir water cover area by using Equations 1-3.

$$NDWI = \frac{Band_{Green} - Band_{NIR}}{Band_{Green} + Band_{NIR}} \tag{1}$$

$$MNDWI = \frac{Band_{Green} - Band_{MIR}}{Band_{Green} + Band_{MIR}}$$
 (2)

$$NDWI = \frac{Band_{Green} - Band_{NIR}}{Band_{Green} + Band_{NIR}}$$
(1)

$$MNDWI = \frac{Band_{Green} - Band_{MIR}}{Band_{Green} + Band_{MIR}}$$
(2)

$$RmNDWI = \frac{Band_{Red} - Band_{MIR}}{Band_{Red} + Band_{MIR}}$$
(3)

The spectral indices value discussed above vary within the range of -1 to +1. The negative value indicates a land area or non-water region. The value close to 0 suggest a saturated water body with a shallow depth, while a value close to 1 indicate a water body with greater depth (Gao, 1996).

4.2 Validating inundation area maps

The water cover areas of the Pong Dam have been extracted for different years with above above-stated indices and further compared with the extracted values by applying the polygon method on historical images received from Google Earth. This approach refers to the quantitative difference between the actual area (using the polygon method from Google Earth) and the estimated area (using water extraction indices from a satellite image) by using Equation 4. Here, the actual area is the base of validation. Due to no alternative source of ground truth data other than Google Earth images for past years, this method is sufficient for real-time visual interpretation. Here, the calculated output would be

$$V_{image-based} = \begin{cases} RA_{actual} - RA_{estimated} = d_0 \\ RA_{actual} - RA_{estimated} = d_1 \end{cases}$$
 (4)

Where, $V_{image-based}$ = Image-based validation; RA_{actual} = Actual reservoir area (km²) derived from water extraction indices; RA_{estimated} = Estimated reservoir area (km²) from Google Earth image; d_0 = the value is close to zero suggest more accurate; d_1 = the value is far from zero suggest less accurate (positive or negative).

For the point-based accuracy assessment, 132-150 reservoir sites were selected from Google Earth images spanning 3 years (2004, 2014, and 2020). In the most recent year (2024), 68 reservoir sites were randomly taken from the field survey. Using this data, overall accuracy and the Kappa coefficient (K) (Monserud and Leemans, 1992) were calculated for all the utilized indices (Equation 5).

$$Kappa (K) = \frac{P\sum_{i=1}^{r} x_{ii} - \sum_{i=1}^{r} (x_{i+} \times x_{+i})}{P^2 - \sum_{i=1}^{r} (x_{i+} \times x_{+i})}$$
 (5)

where P refers to the total number of pixels; r refers to the number of rows in the matrix; Xii is equal to the number of observations in row i and column ii, and xi+ and x + i refer to the marginal totals for row i and column i.

4.3 Computing the hydrological consistency of the reservoir and its seasonal/ temporal dynamics

Hydrological consistency signifies the frequency of water presence in each pixel (Borro et al., 2014) within a reservoir domain, and it is very useful for monitoring hydrological dynamics. This information is vital for identifying stable and unstable parts of water bodies on a seasonal and temporal scale. The area characterised by irregular water presence can be considered as hydrologically vulnerable (Sarda and Das, 2018). For hydrologically consistent area mapping, the time series MNDWI water index maps were used for both pre- and post-monsoon seasons. The reservoir water domain mappings were converted into binary maps, providing 1 to the water and 0 to non-water pixels. Binary maps of all the selected years were summed and divided by the number of years considered for the calculation (Equation 6). It could be expressed in percentages (0%-100%). The hydrological consistency value close to 100% indicates that the presence of water in a pixel is almost consistent. This approach has been successfully employed by several researchers for mapping hydrological consistency of wetlands (Borro et al., 2014; Das and Pal, 2017; Saha et al., 2024). Further, it was classified into five classes, such as Very High (>80%), High (60%-80%), Moderate (40%-60%), Low (20%-40%), and Very Low (<20%). The class belongs to Very High and Very Low in both seasons can confirm the high and low hydrological consistency respectively. Additionally, to examine the

transformation of the hydrological consistent area, the 30 years were divided into three phases, e.g., Phase-1 (1994–2004), Phase-2 (2005–2014), and 2015–2024 as Phase-3. A change detection technique was applied between Phase 1 (1994–2004) and Phase 2 (2005–2014), and between Phase 2 (2005–2014) and Phase 3 (2015–2024) to investigate the temporal shift of areas among the classes of hydrological consistency.

$$HC_j = \frac{\sum_{i=1}^n W_j}{n} \times 100 \tag{6}$$

 HC_j = Hydrological Consistency of jth pixels in a period; $W_j = j^{th}$ pixel having water in the selected MNDWI images; n = number of images.

4.4 Computing the relative water depth of the reservoir and its dynamics

The hydrological consistency (HC) method is an alternative approach for mapping consistent water cover area by utilizing the frequency of water presence (Taheri Dehkordi et al., 2022). This technique only shows the spatial extent of a water body, but does not capture the variations in the water depth (intensity of MNDWI score) for each pixel during the study years. Generally, the value (for a water body) varies from 0 to 1. Where '1' represents high-level water presence and a higher depth of water within the water bodies. The Water Indices score cannot offer a definite water depth, but qualitatively, it represents the equivalent (Gao, 1996). Several studies have found a linear relationship between the intensity of water indices scores and water depth in similar environments (Talukdar and Pal, 2019; Debanshi and Pal, 2020; Pal and Sarda, 2022). However, High eutrophication and turbidity may interrupt the straightforward relation many times (Talukdar and Pal, 2019). In this study, the spectral water index score is considered as a proportional representation of the reservoir's relative water depth. Equation 7 was used to quantify the phase-wise relative water depth over the Pong reservoir.

$$RWD = \frac{\sum_{i=1}^{n} I_x}{N} \tag{7}$$

Where RWD denotes the relative water depth of the reservoir; I_x the images used in an x-th period; N is the total number of years taken into consideration.

For a better understanding of the relative water depth dynamics, the Coefficient of Variation (CV) approach has been used. This approach simply calculates the fluctuation in the Modified Normalized Difference Water Index (MNDWI) score for each pixel, as described in Equation 8. This section focuses on the internal dynamics of relative water depth within the reservoir. It is logically suggested that the pixels exhibit minimal variations in the MNDWI score, represent the hydrologically stable area of the reservoir. Conversely, unstable areas show significant fluctuations in the MNDWI score. Such unstable regions in the reservoir are vulnerable to hydrological and ecological sustainability. For instance, a pixel that retains a deeper water depth 1 year may completely dry out the next year, leading to a higher CV value. In contrast, pixels with consistently show either high or low MNDWI

values are expected to have a low CV score. This analysis indicates stable or unstable reservoir areas, which are critical for the sustainability of species adapted to those specific hydrological conditions.

$$CV = \frac{\sigma}{\mu} \times 100 \tag{8}$$

Where, σ is the standard deviation, μ refers mean score of a given period of the dataset

The above-mentioned approach captures the degree of fluctuation, which signifies the level of consistency, but cannot portray the trend of relative water depth over the region. Therefore, linear regression trend modelling can be adopted to bring out the trend. Here, the pixel-wise linear regression model (Equation 9) has been run in the water body pixels to show the degree of change. It is a very simple and effective way to measure, which focuses on the time series spatial data. This method was successfully applied for detecting the trends of surface water depth in the wetlands (Debanshi and Pal, 2020; Paul and Pal, 2020).

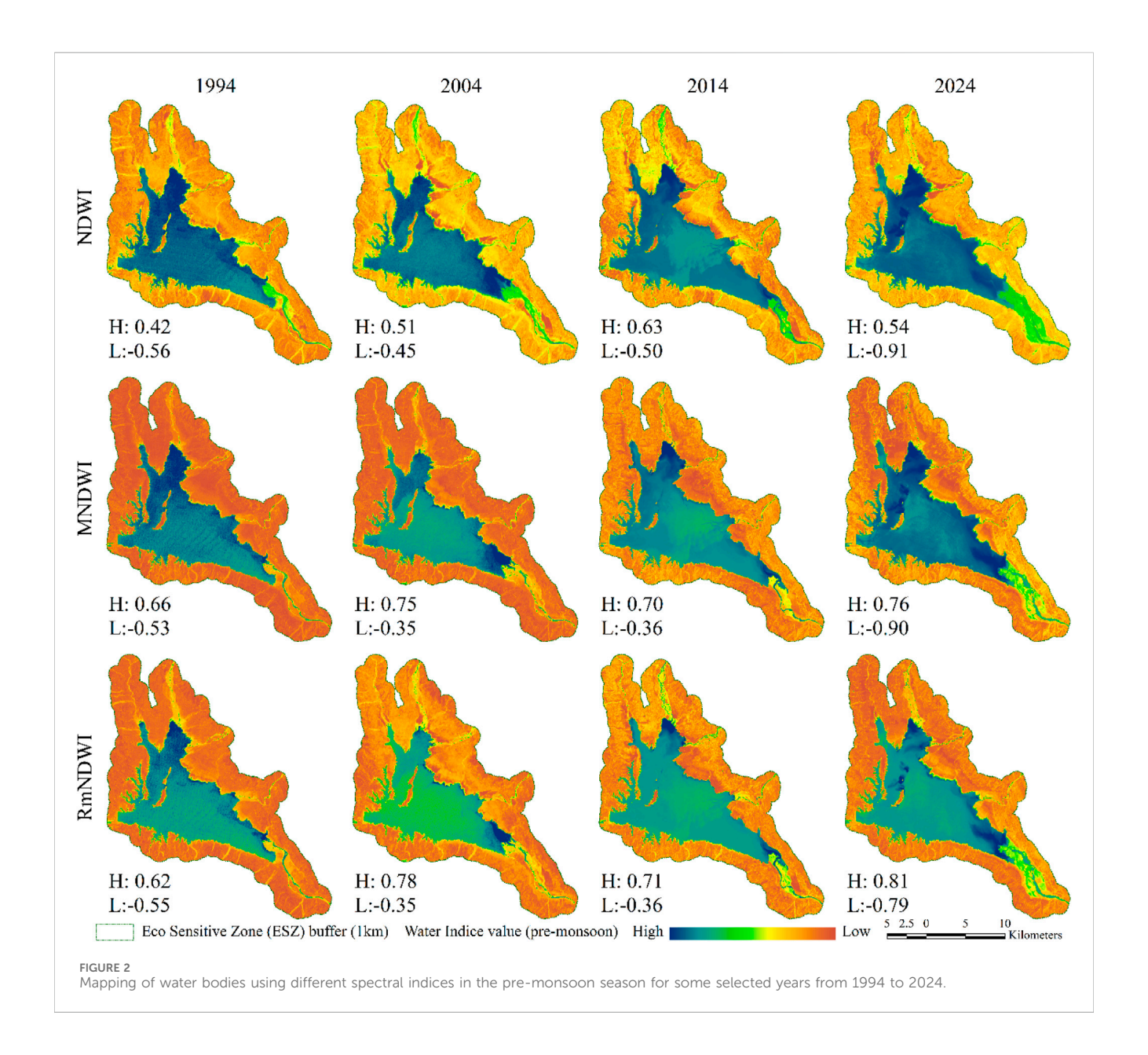
$$Yc = \alpha + \beta X \tag{9}$$

Regression slope (b) and coefficient of determination (R^2) have also been computed for each pixel, which shows the direction and degree of change in the MNDWI score. A high R^2 value indicates a strong change in the MNDWI score over the period, which also indicates the change in the thickness of water in the reservoir. But no studies have been conducted so far on the application of reservoir water state monitoring. Therefore, to the best of the authors' knowledge, the present study was the first study that utilized a spatial trend model for assessing the reservoir hydrological condition at the pixel scale. This analysis provides a quantitative assessment of the overall hydrological condition of a reservoir system.

5 Result and analysis

5.1 Spatio-seasonal inundation area dynamics and its validation

Figures 2, 3 show the delineation of water bodies based on different types of water body extraction indices like NDWI, MNDWI, and RmNDWI in the range of 10 years (1994, 2004, 2014, and 2024) for pre- and post-monsoon seasons. Essentially, this method is effective on satellite imagery. Consequently, these kinds of water extraction indices were separated by water body and nonwater body in a certain numerical range, and those values can be either positive or negative. The areal pattern of the water spread area was mapped by those three water extraction indices. The postmonsoon season recorded maximum spatial water coverage compared to the pre-monsoon season. In each year, NDWI indices reflect the low areal extent compared to the other two indices (MNDWI and RmNDWI), where MNDWI spectral indices show maximum wetland areal coverage. For example, in 1994, the water cover areas during pre- and post-monsoon seasons were 134.60 km² and 229.96 km² respectively. While in 2004, the areal extent were 137.62 and 186 km², and in 2024, it stands



123.80 km² and 223.26 km² (Table 2). Since rainfall and river inflow are the main sources of reservoir water, based on seasonal variability of rainfall, a significant difference in water cover area within the reservoir was recorded between pre- and post-monsoon seasons.

Two types of validation approaches (image-based and point-based) were conducted for accuracy assessment of three water indices maps (NDWI, MNDWI, RmNDWI). In the image-based approach, the actual water cover area was digitized using Google Earth Pro images for the accuracy of the water spread area. The actual area was then compared to the areas determined by the water extraction indices. The reservoir water cover areas extracted through the polygon method from Google Earth images were 175.88 km², 202.74 km², 220.88 km² and 228.66 km² for the years 2004, 2014, 2020 and 2024 respectively. Table 3 depicts the result of the polygon-based accuracy assessment. The result indicates that the Normalized Difference Water Index (NDWI) performed well, showing a surface water area of 179.78 km² for the year 2004. Further seen in the years

2014, 2020, and 2024 the MNDWI index output (193.69 km 2 , 217.85 km 2 , and 233.78 km 2) aligns relatively well with the areas identified in Google Earth images.

Table 4 presents the results of the point-based accuracy assessment for various water indices (NDWI, MNDWI, and RmNDWI). In the point-based evaluation, it is clear that all indices accurately depicted the water cover area from 2004 to 2024 across both seasons. The level of correspondence between the map and actual conditions ranges from good to excellent for all the indices. Comparing the extracted results using different indices, it was determined that the MNDWI method is the most suitable for mapping water coverage in the reservoir. While MNDWI is structurally similar to NDWI, it utilizes the shortwave infrared (SWIR) band instead of the near-infrared (NIR) band. This adaptation makes MNDWI an improvement over NDWI, as water features absorb more energy in the SWIR band (Xu, 2006). Further studies were conducted using the MNDWI water index.

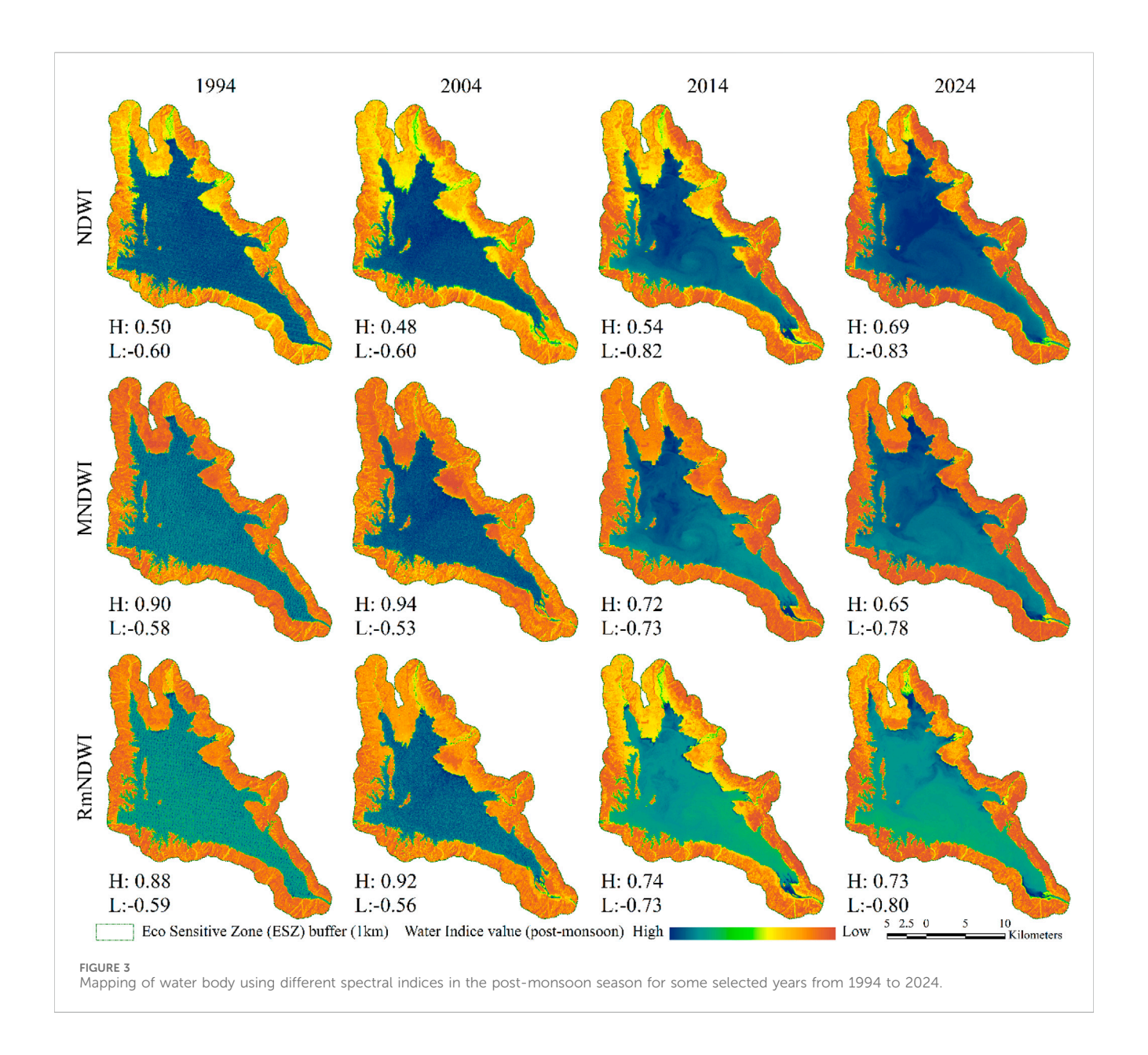


TABLE 2 Areal statistics of the Pong reservoir for pre- and post-monsoon seasons.

Year	Area (Km²) for the pre-monsoon season			Area (Km²) for the post-monsoon season			
	NDWI	MNDWI	RmNDWI	NDWI	MNDWI	RmNDWI	
1994	138.67	134.60	135.20	231.33	229.96	228.75	
2004	144.03	137.62	149.19	179.78	186.00	182.49	
2014	151.75	153.90	153.03	191.28	193.69	192.35	
2024	112.97	123.80	122.74	220.35	223.26	222.79	

5.2 Trend of the inundation area and seasonal water depth

Seasonal and temporal variations in inundation area and intensity of MNDWI were observed through time series analysis. The findings indicated that the inundation area, maximum and average MNDWI

intensity exhibited a declining trend from 1994 to 2024 during both preand post-monsoon periods (Figure 4). The trends for maximum MNDWI value (excluding pre-monsoon) and average MNDWI value were determined to be negative, with a probability value of less than 0.05 for both pre- and post-monsoon seasons. A reduction in the maximum MNDWI value either indicates increased

TABLE 3 Accuracy assessment result of the polygon-based approach using Google Earth images.

Year	Actual area (km²)	Estimated area (km²)						
	Google earth images	NDWI		MNDWI		RmNDWI		
		Area	Difference	Area	Difference	Area	Difference	
2004	175.88	179.78	-3.9	186	-10.12	182.49	-6.61	
2014	202.74	191.28	11.46	193.69	9.05	192.35	10.39	
2020	220.88	211.82	9.06	217.65	3.23	213.88	7	
2024	228.66	220.35	8.31	223.26	5.4	222.69	5.97	

TABLE 4 Overall accuracy and kappa statistics of water coverage area for pre- and post-monsoon seasons.

Year	Indices	Pre-m	nonsoon	Post-monsoon		
		Overall accuracy	Kappa Co-efficient	Overall accuracy	Kappa Co-efficient	
2004	NDWI	93.77	0.87	91.67	0.87	
	MNDWI	95	0.89	96	0.92	
	RmNDWI	95	0.89	94	0.89	
2014	NDWI	91.33	0.82	94	0.88	
	MNDWI	95	0.92	95.33	0.9	
	RmNDWI	94	0.91	94	0.9	
2020	NDWI	91	0.85	92	0.85	
	MNDWI	96.61	0.9	95	0.91	
	RmNDWI	93	0.87	93	0.87	
2024	NDWI	93	0.84	91	0.88	
	MNDWI	96.56	0.93	97	0.94	
	RmNDWI	94	0.9	95.5	0.92	

sedimentation or a contraction in the water-covered area. This also demonstrated a reduction in relative water depth over time. Although the water-covered area displayed temporary fluctuations, but its overall trend has been negative in both the pre-monsoon and post-monsoon seasons over the past 30 years, suggesting a reduction in water availability within the reservoir.

There were noticeable fluctuations in the reservoir area for both pre- and post-monsoon seasons. This section also presents phasewise changes in the seasonal area of the reservoir. From the result, it was evident that the areal fluctuations ranged from 7% to 27% for pre-monsoon and post-monsoon seasons respectively (Table 5). During the pre-monsoon season, the average area was 158.59 km² in Phase-1 (1994–2004), which reduced to 137.66 km² in Phase-3 (2015–2024). A similar declining trend was observed in the post-monsoon season, where the average area was approximately 219.04 km² in Phase-1, but it stands at 212.13 km² in the recent phase (2015–2024). Table 4 also depicts that in the post-monsoon season, the coefficient of variation (CV) value was lower than the pre-monsoon season due to the higher concentration of rainfall during the monsoon season, which primarily contributed to filling the reservoir area.

5.3 Anomaly of reservoir area and the intensity of MNDWI score

Anomaly detection is a widely used technique employed by many researchers to address the extreme occurrences in long-term time series datasets (Saini et al., 2020; Soriano-Vargas et al., 2021). To identify an anomaly, a minimum of 30 years of data is typically required, as shorter datasets may not capture the signals of variability (Stevens-Rumann et al., 2018). Figure 5 provides a visual representation of long-term anomalies in maximum MNDWI score, average MNDWI score, and inundation area for both pre-and post-monsoon seasons from 1994 to 2024. Positive anomaly values are higher than the long-term average value, while negative anomaly value denotes the opposite and vice versa. The deeper part of the reservoir is identified by the maximum MNDWI score. The anomaly value for the maximum MNDWI score ranges from -2.33 to 2.61 and -1.57 to 2.48 in pre-and post-monsoon seasons. A good many years registered a positive anomaly of average MNDWI; however, after 2012, all the years recorded a significant reduction of average MNDWI score with a negative anomaly. The drastic reduction (anomalies) was observed in both pre-and post-

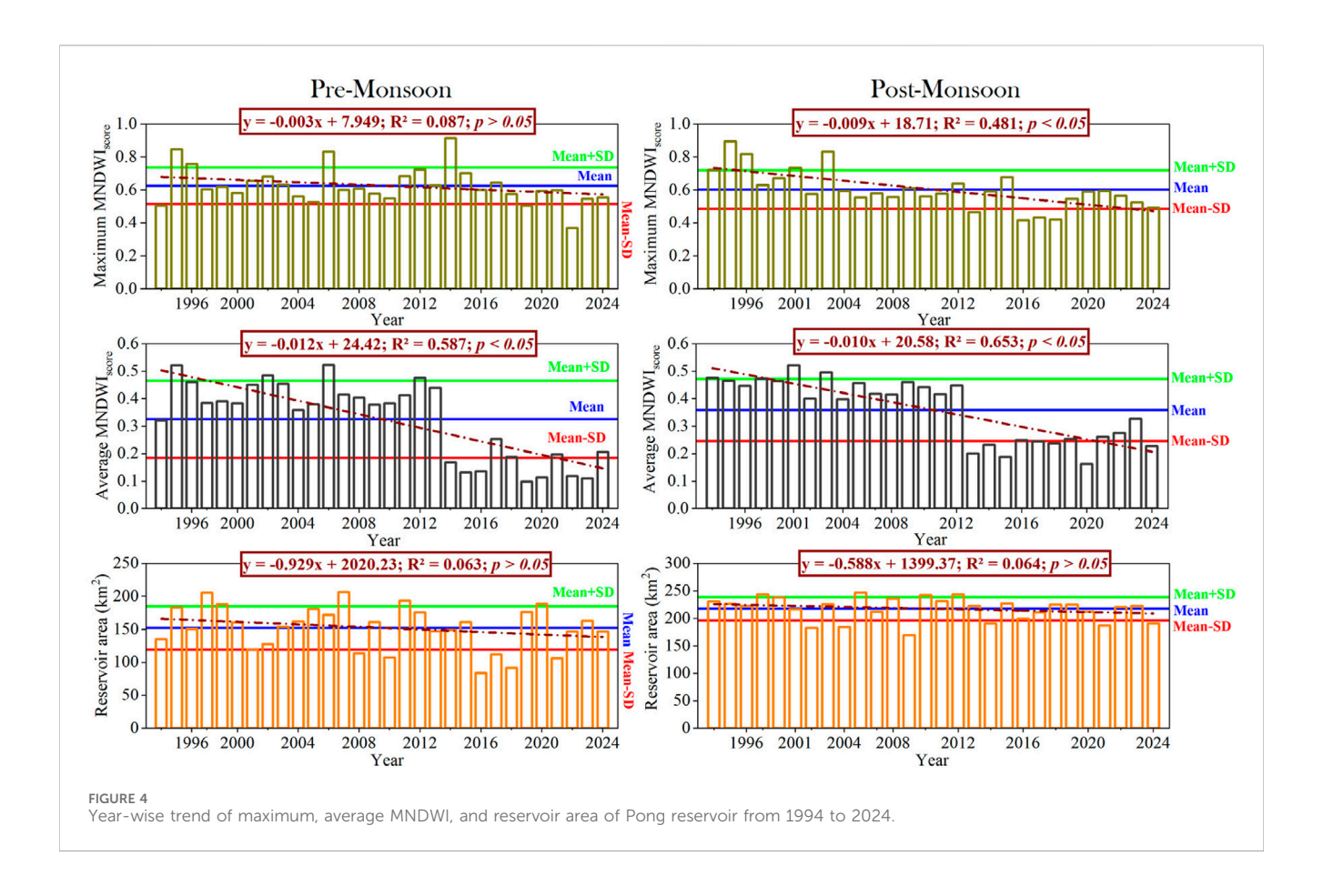


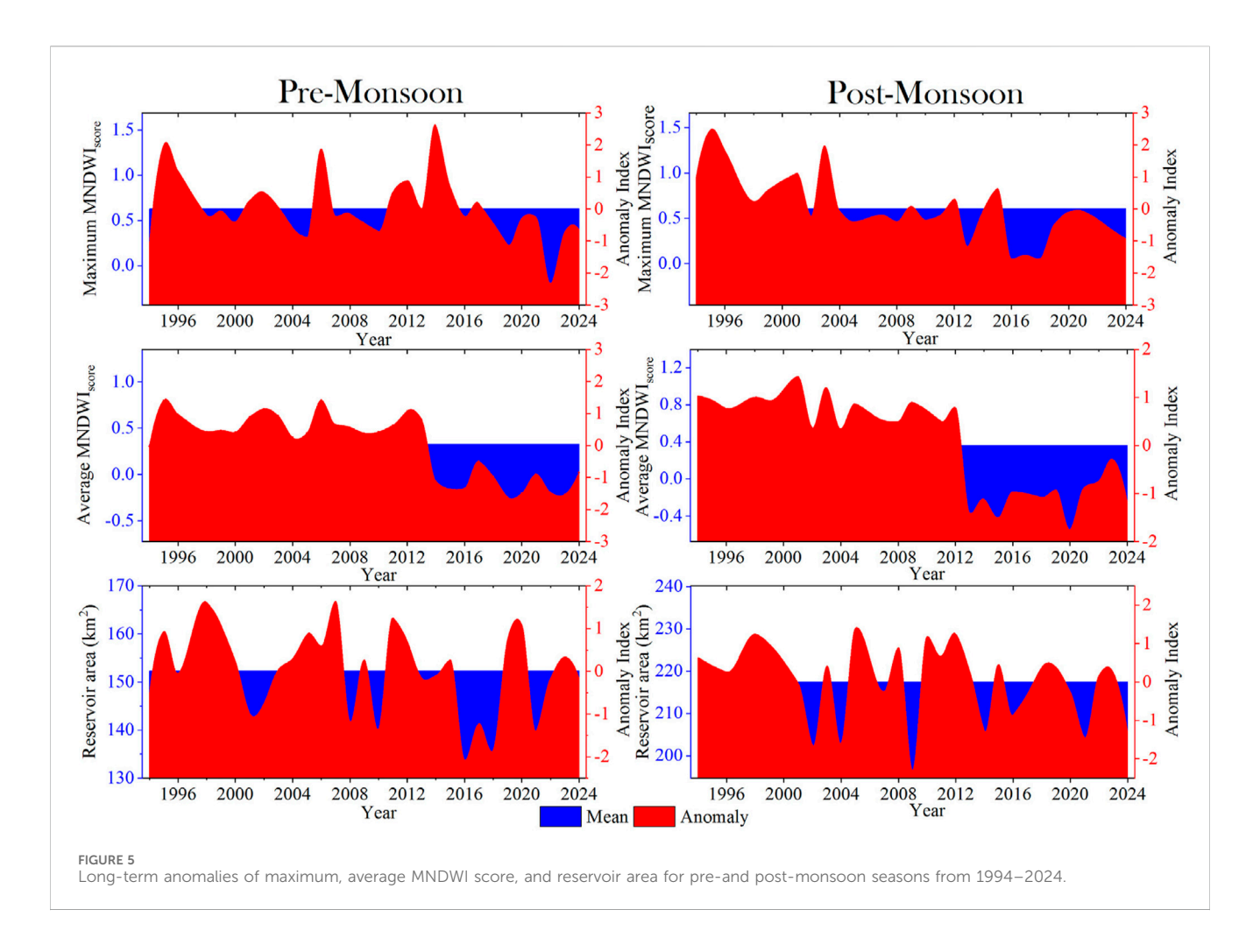
TABLE 5 Phase-wise seasonal areal fluctuation analysis of Pong reservoir.

Season	Period	Average area (km²)	CV (%)	Yc = a+bx	R ²
Pre-monsoon	1994-2024	152.29	21.65	y = -0.9296x + 2020.2	0.06
	1994-2004	158.59	17.31	y = -1.633x + 3423.4	0.04
	2005-2014	160.64	20.07	y = -2.5819x + 5348.9	0.06
	2015-2024	137.66	26.71	y = -4.0075x - 7955.6	0.11
Post-monsoon	1994-2024	217.44	9.64	y = -0.5881x + 1399.4	0.06
	1994-2004	219.04	9.87	y = -3.6492x + 7514.1	0.37
	2005-2014	221.73	11.97	y = -2.0238x + 4289.4	0.05
	2015-2024	212.13	7.06	y = -1.4637x + 3168	0.09

monsoon seasons. This indicates a sharp decline in the relative water depth of this reservoir, which is a major concern for the long-term operation of the reservoir. The anomaly value ranges from -1.41 to 1.62 for pre-monsoon and -1.75 to 1.44 for post-monsoon seasons. Seasonal variation of the reservoir water coverage area was also very evident from Figure 5. However, the yearly fluctuation of the inundation area and the frequency of negative anomalies were maximum in recent years for both seasons. The anomaly value (reservoir area) ranges from -2.08 to 1.65 for the pre-monsoon and -2.30 to 1.40 for the post-monsoon season. This suggests that the water coverage area of the reservoir declined over the period (1994–2024).

5.4 Spatio-seasonal hydrological consistency of the reservoir

The water body for each year has been composited to show the pixels where it appears either consistent or inconsistent. It is assumed that if a pixel shows a water body frequently, it qualifies as a hydrologically consistent area. Based on this approach, Hydrological consistency has been calculated for both the premonsoon and post-monsoon seasons, as displayed in Figure 6. To enhance clarity, each map has been categorized into five classes: very high, high, moderate, low and very low. The very high zone is considered hydrologically and ecologically sustainable,



whereas the very low zone is prone to issues with water retention. Variability in rainfall and river flow might contribute to the increase in the wetted area of the reservoir through inflow and outflow operations. Figure 6 shows the phase-wise hydrological consistency of the Pong reservoir in pre- and post-monsoon seasons from 1994 to 2024. From the years 1994-2024, out of the total area, 5% and 9% of areas were recorded as having very low hydrological consistency (below 20%), which is susceptible to conversion in both pre-and post-monsoon seasons. Only about 25% and 42% of areas were recorded as very high (above 80%) hydrologically consistent areas. The outcomes indicate that the reservoir can be considered reliable for water-based planning in both seasons. The analysis of hydrological consistency clearly shows that the outer part or fringe area of the reservoir was gradually losing its consistent characteristics, particularly during the pre-monsoon season. The situation of hydrological consistency in the post-monsoon season was quite different from the pre-monsoon season. The result shows that hydrological consistency within the reservoir would be high in the post-monsoon season. Table 6 depicts the phase-wise areal extent of reservoir areas under different hydrological consistency classes for pre- and post-monsoon seasons. In the recent phase (2015-2024), the total area classified as having very high consistency was 88.49 km², indicating a reduction of about 36% from Phase-1 (1994-2004) during the pre-monsoon season. Conversely, the area classified as having very high consistency in the post-monsoon season showed a slight increase (about 1%). However, there was a significant reduction of about 40% in the area classified as high consistency over the past 30 years during the post-monsoon season. The proportion of area under the very low hydrological consistent zone was found to be drastically reduced (about 64%), against the general trend, which was practically due to the complete wiping out of a wider part of the fringe reservoir area in the post-monsoon season. It does indicate growing hydrological uncertainty in the reservoir. An increase in uncertainty implies a growing vulnerability in water storage. The rising inconsistency across a larger reservoir area raises concerns regarding the future reliability of water supply from the reservoir.

5.5 Phase-wise changes in the hydrological consistency character of Pong reservoir

To better understand the changes in hydrological classes between Phase-1 (1994–2024) and Phase-2 (2005–2014), as well as between Phase-2 and Phase-3 (2015–2024), a change detection analysis was conducted. The results are illustrated in Figure 7, while Table 7 presents the areal transformations from one consistency class to another for each phase. In the pre-monsoon season, approximately 158.24 km², representing 72%, and 121.22 km², or 55%, of the wetland area remained unchanged in terms of

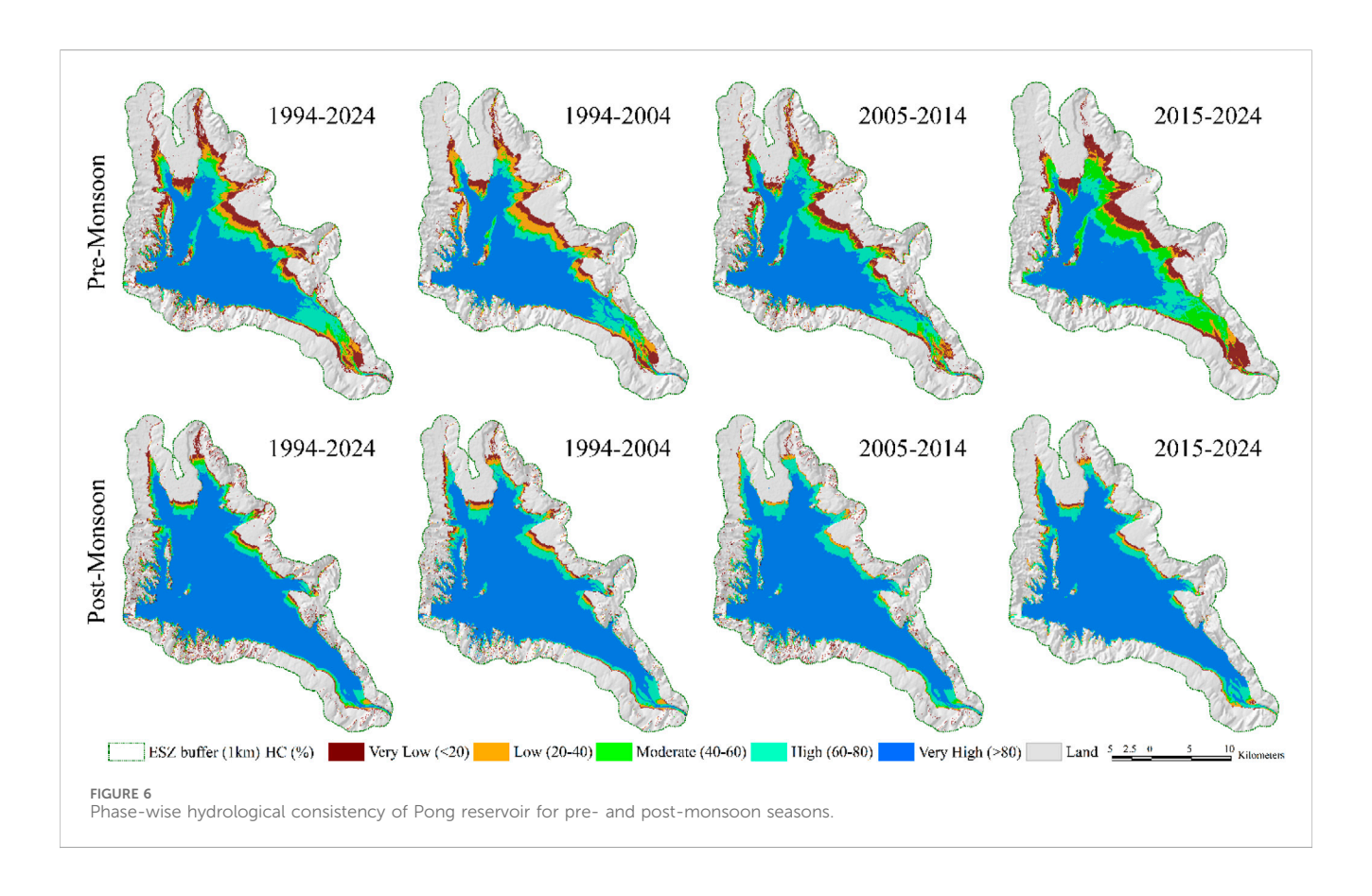
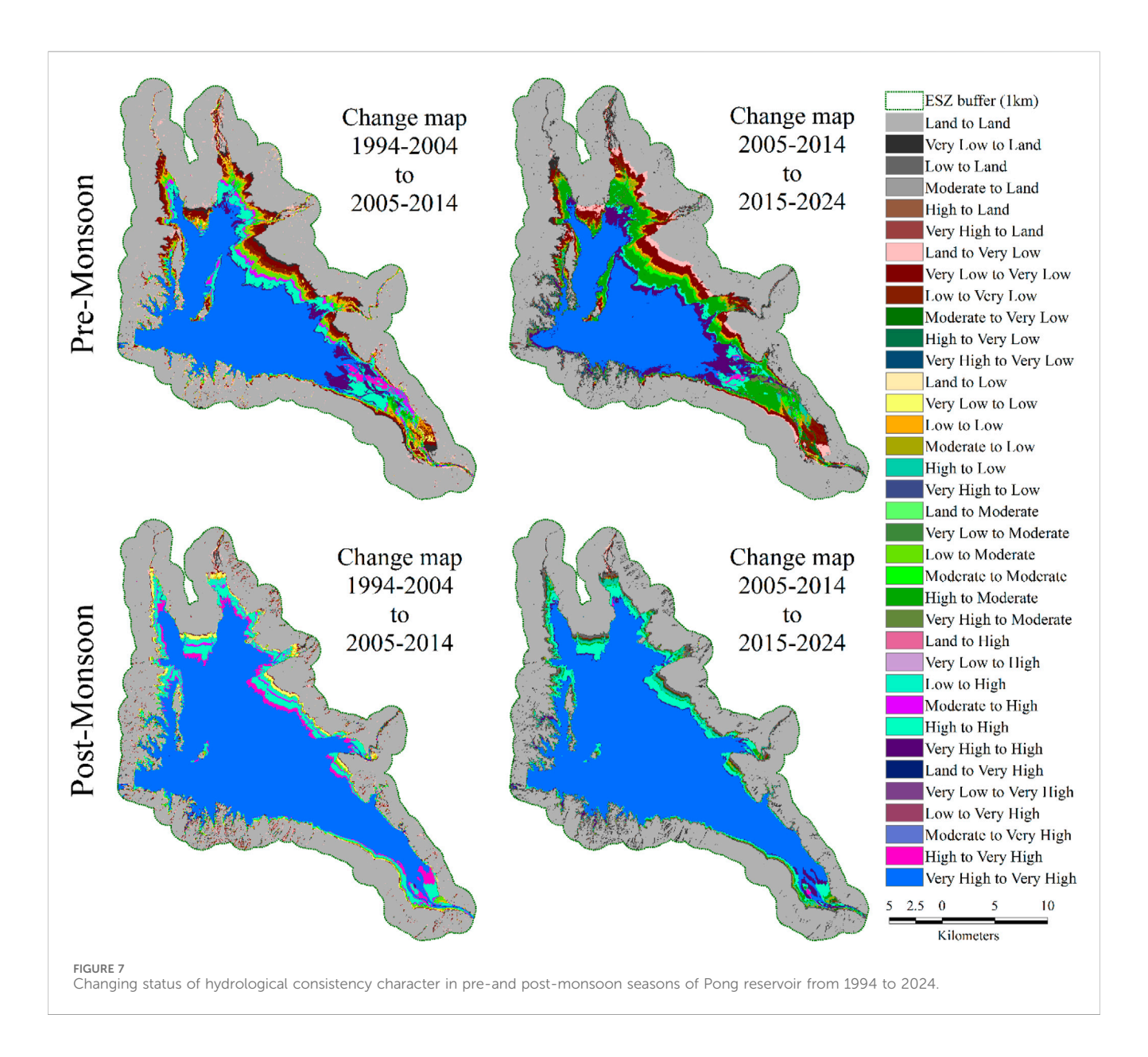


TABLE 6 Season-wise areal extent of different hydrological consistency classes.

Season	Hydrological consistency	1994–2024		1994-2004		2005–2014		2015-2024	
	class (%)	Area (km²)	in %						
Pre-Monsoon	Land	242.32	52.12	254.04	54.65	251.64	54.13	263.32	56.64
	Very Low (<20)	39.64	8.53	25.36	5.45	32.52	6.99	37.26	8.01
	Low (20-40)	21.12	4.54	27.73	5.96	12.73	2.74	13.36	2.87
	Moderate (40–60)	13.94	3.00	11.48	2.47	15.63	3.36	35.35	7.60
	High (60–80)	33.32	7.17	25.73	5.53	39.79	8.56	27.11	5.83
	Very high (>80)	114.53	24.64	120.54	25.93	112.58	24.22	88.49	19.04
Post-	Land	206.14	44.34	211.25	45.44	210.01	45.18	234.03	50.34
Monsoon	Very low (<20)	23.00	4.95	17.45	3.75	12.83	2.76	6.33	1.36
	Low (20-40)	9.45	2.03	13.16	2.83	10.12	2.18	10.68	2.30
	Moderate (40-60)	12.23	2.63	4.79	1.03	6.86	1.48	4.64	1.00
	High (60–80)	20.93	4.50	34.87	7.50	33.94	7.30	24.91	5.36
	Very high (>80)	193.14	41.55	183.37	39.44	191.12	41.11	184.29	39.64

Hydrological Consistency (HC) character. About 12.44 km 2 (Phase-1 to Phase-2) and 55.87 km 2 (Phase-2 to Phase-3) of very high and high hydrologically consistent wetland areas were transformed into relatively lower categories in the pre-monsoon season. About 32.68 km 2 of area in the pre-monsoon season was recorded,

where hydrological consistency was improved from Phase 1 to Phase 2. But in the next cycle (Phase-2 to Phase-3), it was reduced significantly, and about 8.77 km² of the area maintained the improvement in their hydrological consistency. Qualitative degradation of the hydrological consistency was more prominent



in the outer areas of the reservoir. This fact was also true for the postmonsoon season. For the post-monsoon season, 3.72 km² and 24.24 km² areas were drastically wiped out (converted to land) from Phase-1 to Phase-2 and from Phase-2 to Phase-3. The hydrologically consistent area of the reservoir in the postmonsoon season was more stable than in the pre-monsoon season. Unchanged hydrological consistency areas were respectively 211.33 km² and 202.56 km². From the hydrological consistency change matrix, it was clear that over time, the transformation of consistency from higher to lower is about 10.62 km² and 51.97 km² in the post-monsoon season. Only 36.65 km² area noticed positive changes in the hydrological consistency category between Phase-1 to Phase-2. No significant evidence was found indicating any improvement in hydrological consistency from Phase-2 to Phase-3. Figure 8 displays the areal transformation (in percentage) of hydrological consistency classes for pre- and post-monsoon seasons. These transformations in hydrological consistency are likely to have a substantial impact

on the ecological efficiency and overall health of the reservoir's ecosystem.

5.6 Relative water depth dynamics of Pong reservoir

Figure 9 illustrates the dynamics of relative water depth over the different phases. The relative water depth of the reservoir was analysed based on the change of MNDWI intensity over the reservoir. The fluctuation of MNDWI intensity serves as a critical indicator of the reservoir ecosystem's health. Figure 9 shows that in Phase-3 (2015–2024), the average MNDWI score was reduced to 0.15 from 0.39 in the pre-monsoon season. This reduction in MNDWI intensity indicates a qualitative degradation of the wetland concerning water thickness. Conversely, an increase in MNDWI intensity would signify an improvement in the water depth. The result also stated that for the post-monsoon season,

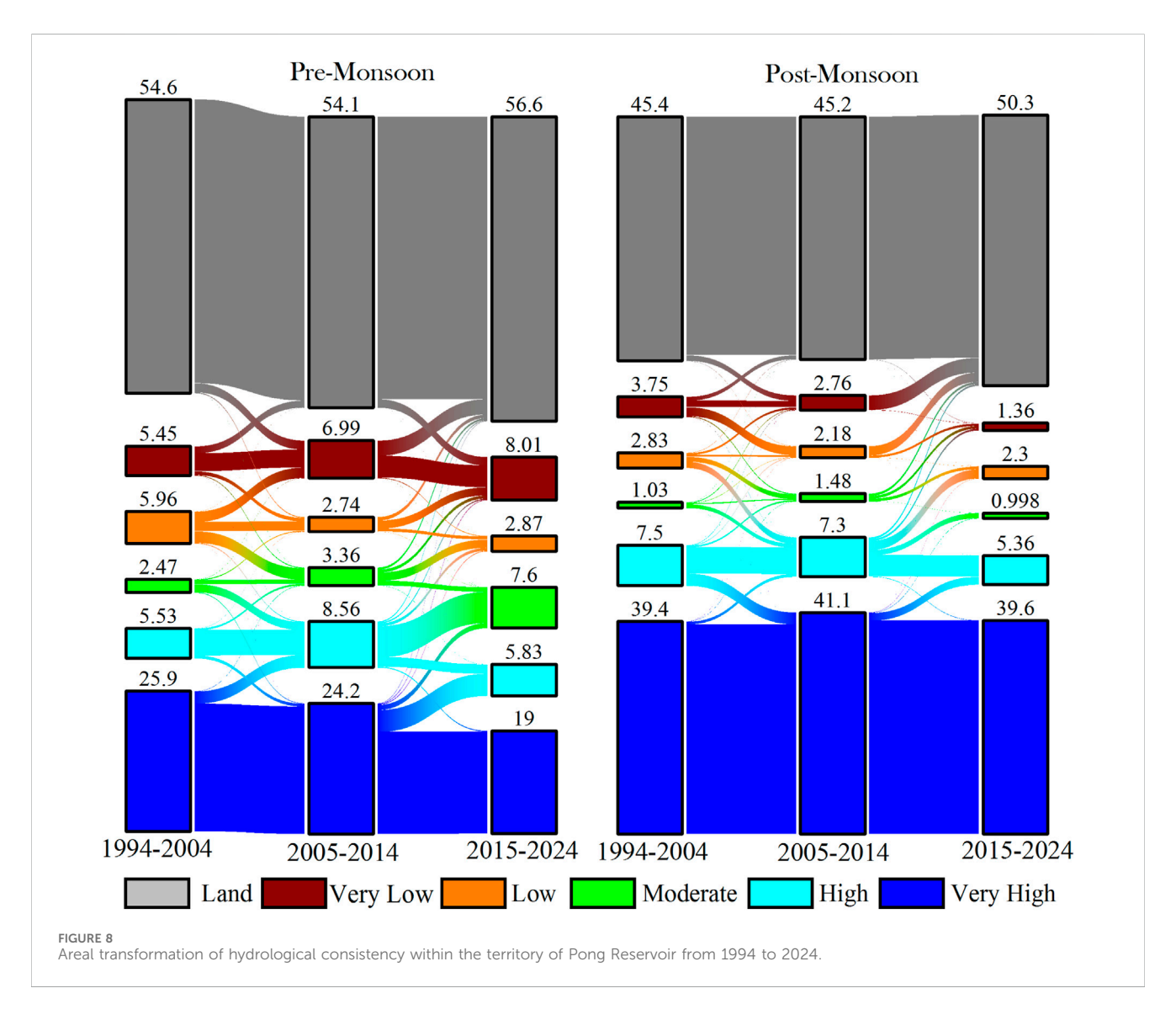
TABLE 7 Areal extent of changes in hydrological consistency characters of pre-and post monsoon seasons.

Category	Changes in HC classes	Pre-mo	onsoon	Post-monsoon			
	HC Classes	From 1994–2004 to 2005–2014	From 2005–2014 to 2015–2024	From 1994–2004 to 2005–2014	From 2005–2014 to 2015–2024		
		Area in sq km					
Unchanged	Land to Land	245.46	244.29	206.28	209.79		
	Very Low to Very Low	15.50	18.88	5.58	0.18		
	Low to Low	8.01	2.57	1.5	0.08		
	Moderate to Moderate	3.42	3.96	0.81	0.05		
-	High to High	21.66	8.01	22.69	18.25		
	Very High to Very High	109.65	87.79	180.75	184		
Changes in Very	Very High to Land	0.00	0.33	0	0.01		
High	Very High to Very Low	0.00	0.44	0.02	0.02		
	Very High to Low	0.01	0.61	0.1	0.23		
	Very High to Moderate	0.22	4.42	0.14	0.22		
	Very High to High	10.66	18.99	2.36	6.64		
Changes in High	High to Land	0.00	0.71	0.01	1.5		
	High to Very Low	0.01	1.01	0.27	1.66		
	High to Low	0.13	2.52	0.37	7.87		
	High to Moderate	1.42	26.84	1.18	4.36		
	High to Very High	2.51	0.69	10.36	0.29		
Changes in Moderate	Moderate to Land	0.00	1.80	0.04	2.01		
Moderate	Moderate to Very Low	0.13	2.61	0.46	2.32		
	Moderate to Low	0.70	7.15	0.26	2.46		
	Moderate to High	6.84	0.10	3.21	0.01		
	Moderate to Very High	0.39	0.00	0	0		
Changes in Low	Low to Land	0.07	3.080	0.27	8.09		
	Low to Very Low	9.05	6.984	1.74	1.95		
	Low to Moderate	9.96	0.086	4.06	0		
	Low to High	0.61	0.002	5.59	0		
	Low to Very High	0.02	0.001	0	0		
Changes in Very Low	Very Low to Land	6.11	13.11	3.4	12.63		
very Low	Very Low to Low	3.17	0.49	7.7	0.02		
	Very Low to Moderate	0.56	0.03	0.67	0		
	Very Low to High	0.02	0.01	0.1	0		

(Continued on following page)

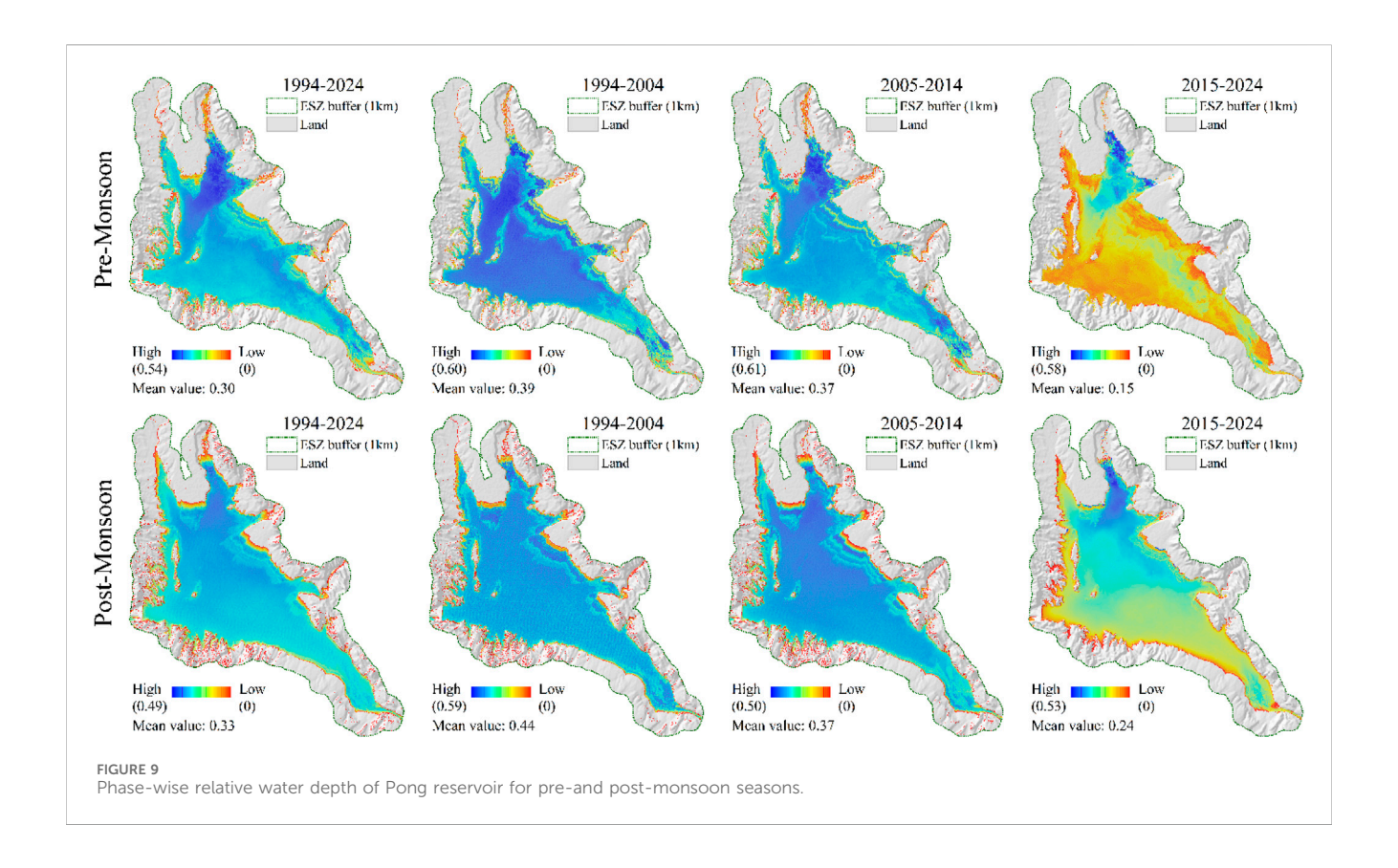
TABLE 7 (Continued) Areal extent of changes in hydrological consistency characters of pre-and post monsoon seasons.

Category	Changes in HC classes	Pre-mo	onsoon	Post-monsoon		
	TC Classes	From 1994–2004 to 2005–2014	From 2005–2014 to 2015–2024	From 1994–2004 to 2005–2014	From 2005–2014 to 2015–2024	
		Area in sq km				
	Very Low to Very High	0.00	0.00	0	0	
Land to HC	Land to Very Low	7.84	7.33	4.77	0.2	
classes	Land to Low	0.70	0.02	0.19	0.02	
	Land to Moderate	0.05	0.01	0	0	
	Land to High	0.00	0	0	0	
	Land to Very High	0.00	0	0	0	



the average MNDWI score was 0.44 for the Phase-1 (1994–2004), but it was 0.24 in Phase 3 (2015–2024). This decline reflects a gradual reduction in water thickness, which negatively impacts the

habitat quality. A spatial analysis of relative water depth also exhibited that in the Phase-3, a significant shallowing area was detected in the reservoir fringe area. Additionally, the effects of



temporal distance contribute to the hydrological deterioration of the reservoir.

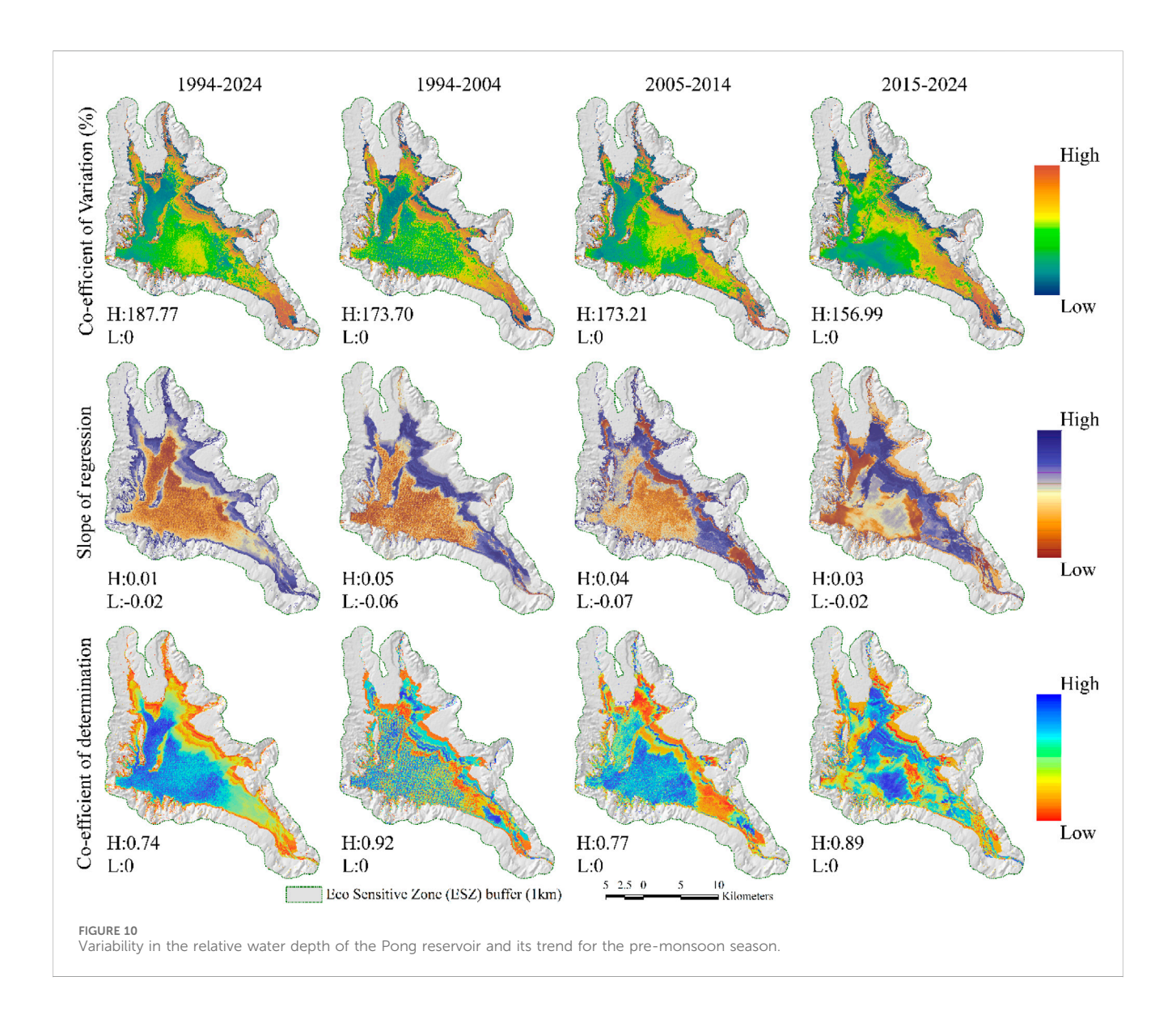
5.7 Hydrological variability and trend in the relative water depth of the reservoir

Season-wise variability of reservoir water thickness was illustrated in Figures 10, 11. The coefficient of variation value (%) ranges from 156.99 to 173.70 for the pre-monsoon season and 163.86 to 186.64 for the post-monsoon season from 1994 to 2024. The reservoir fringe area experienced high variation in the relative water depth. Pixel-wise relative water depth images in the backwatered regions from 1994 to 2024 represent the spatial trend modelling, including the coefficient of determination (R2) and regression slope (b) for pre- and post-monsoon seasons displayed in Figures 10, 11. The trend analysis result revealed that the reservoir core part experienced a negative trend, and the value of the regression slope (b) varies from -0.02 to 0.01, with a coefficient of determination (R^2) varying from 0.74 to 0.85 in the last 30 years (1994-2024) for pre- and post-monsoon seasons. This sort of finding indicates a decreasing trend over time and a quantitatively reduced relative water depth of the reservoir in both seasons. Figures 10, 11 also show the pixel-wise trend of relative water depth for pre- and post-monsoon seasons in different periods. In the 1st, 2nd, and 3rd phases, the computed coefficient of determination varied from 0 to 0.92, 0 to 0.77, and 0 to 0.89 for the pre-monsoon season and 0 to 0.94, 0 to 0.92, and 0 to 0.92 for the post-monsoon season. While the average value was 0.45 in Phase-1 (1994-2004), it stands at 0.50 in Phase-3

(2014-2024). It signifies the progressive trend in the degree of change. In addition to obtaining the direction of change, pixelwise bita value (intercept) was computed for pre- and post-monsoon seasons (Figures 10, 11). From the figures, it was found that peripheral parts of the reservoir exhibited positive change in the pre-monsoon season, but this does not necessarily mean that the water body was stable. This situation happened because it was a transitional part of the reservoir. The core part of the reservoir shows a negative change during the pre-monsoon season over the years, and it is not a good sign from the wetland preservation point of view. The result suggests that the shallow water levels in backwaters were increasing, alongside a growing water scarcity during the premonsoon season. The result further indicates that the intensity of waterlogging depth has changed significantly in the reservoir areas due to anthropogenic and natural factors. Various particles (organic and inorganic) were carried down and deposited along the riverbed. Over time, these particles accumulated in the reservoir area and caused a continuous decrease in its depth. As a result, the water storage capacity was adversely affected.

6 Discussion

The monitoring of hydrological dynamics in the Pong reservoir revealed a reduction in the water cover area and a decline in the hydrological consistency character over time. The study also recorded seasonal variations in shallow water depth within the reservoir. The hydrological consistency of a reservoir is a complex interplay of several interacting factors, including sedimentation, rainfall, and river inflow. However, this study did not examine the role of water inflow into the



reservoir, which remains a critical area for understanding the hydrological dynamics of the reservoir. It is crucial to highlight that the rainfall regime and its seasonal variability play a pivotal role in regulating water influx into the reservoir. Approximately 36.18 km² of the reservoir area was identified as seasonal. Seasonal variability in rainfall is the key factor driving the fluctuations in the water cover area from season to season. Therefore, the trend analysis was performed using linear regression to examine the temporal nature of the seasonal rainfall. For this examination, IMD-endorsed rainfall data (1994-2024) were utilized. This comprehensive dataset provides crucial historical rainfall records across various regions of India, enabling robust longterm trend assessment (Nandi et al., 2024). The result shows that there is no significant trend in the seasonal rainfall over Pong Reservoir (Table 8). Hence, the study extended the analysis to encompass different rainfall indices, which provides a comprehensive view of the rainfall regime of the region (Figure 12). The outcomes show statistically significant decreasing trends in the number of rainy days, maximum consecutive wet days, and total precipitation on wet days. These results suggest that rainfall occurred less frequently over the study period and trends towards shorter wet spells. Interestingly, indices related to extreme rainfall events, such as heavy precipitation days (>64 mm), maximum 1-day rainfall, and maximum 5-day rainfall, did not show any statistically significant trend. These sorts of findings were treated as the major driving factor for reducing flow influx as reported in this present study, which can also contribute to the hydrological consistency of the reservoir. This indicates a complex and potentially unpredictable hydrological future for Pong Reservoir and its surrounding ecosystems.

Besides decreasing the rainfall trend, the reservoir faces challenges associated with sediment influx or escalating sediment deposition. This sedimentation not only obstructs the flow of water but also leads to a gradual decrease in the water depth of the reservoir. The overview of the regression model indicates that the intensity of water logging depth changed over the period (1994–2024). The core area of the reservoir exhibits a discernible trend of relative water depth. Previous literature also reported that gradual siltation of the reservoir bed and loss of water retaining capacity of the same were ensuing problems for the Pong reservoir (Garg and Jothiprakash, 2013; Shukla et al., 2017; Sharma et al., 2021). This sort of finding was further supported by the trend of siltation rate and gross storage of reservoirs in past years based on

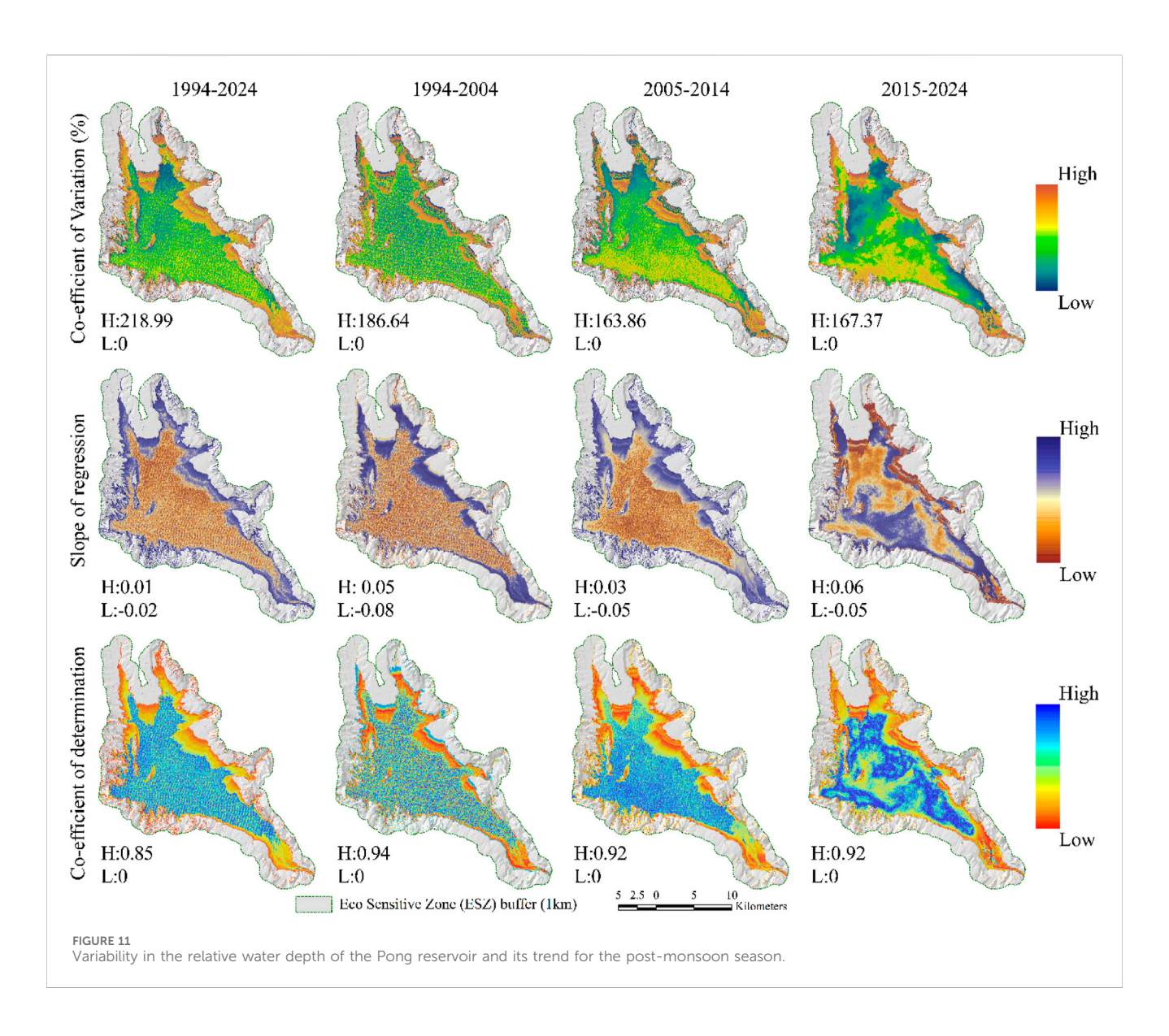


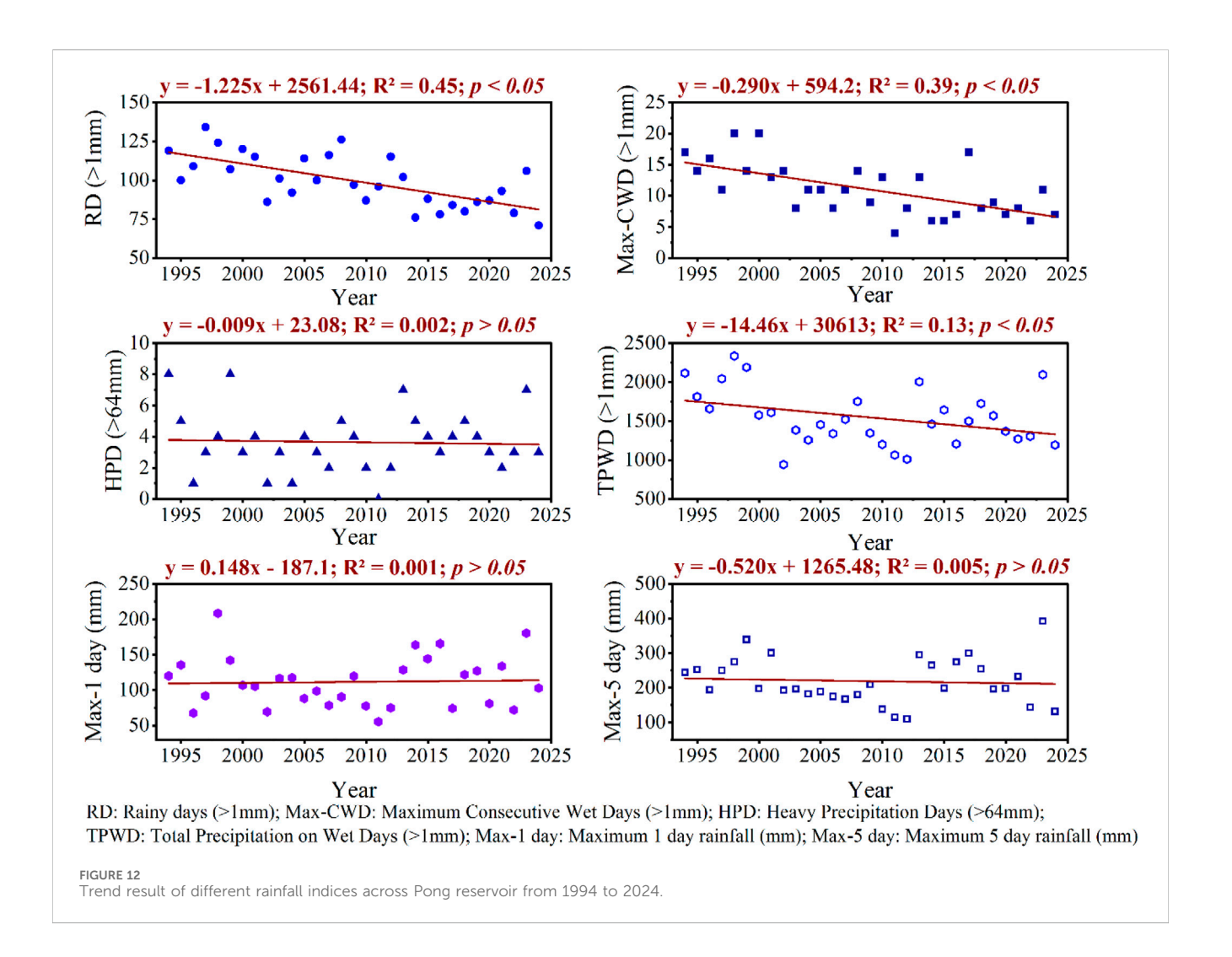
TABLE 8 Seasonal rainfall statistics and their trend over the Pong reservoir.

Season	Mean rainfall (mm)	Standard deviation	Coefficient of variation (%)	Regression	R ²	Remarks
(1994–2024)	raimau (mm)	deviation	variation (%)	equation		
Pre-monsoon	52.99	27.17	51.27	y = 0.105x - 159.5	0.001	Insignificant
Monsoon	297.84	95.51	32.07	y = -3.546x + 7423.	0.114	Insignificant
Post-monsoon	21.95	18.79	85.59	y = 0.094x - 167.6	0.002	Insignificant
Winter	71.59	42.76	59.74	y = -0.470x + 1016.	0.010	Insignificant

the data received from the India WRIS platform. The positive trend of siltation rate (y = 0.0338x + 1.2718; $R^2 = 0.21$) and a negative trend of gross storage area (y = -23.546x + 8049.1; $R^2 = 0.94$) of the reservoir explain the squeeze of relative water depth of the reservoir over the years (1994–2018). The increased siltation rate affects the gross storage of the reservoir, aligning with the previous research by Shukla et al. (2017) and Malik and Rai (2019). They also reported that the rate of sedimentation (varies from 18.08 to 24.40 Mm³/year)

of the Pong reservoir was gradually increasing, which would also lead to a gradual decrease in maximum water depth. This sort of finding signifies the declining trend of water storage, which is against of economic interests of the people. On the other side, changes in water depth can also affect the habitat availability for aquatic life and potentially lead to adverse effects on the local ecosystem.

As the depth of the reservoir continues to decrease, there will be a chance of an extension of the water presence area within the



reservoir. The outcome of this research work is almost identical to the above-stated theoretical expectation because in the postmonsoon season water cover area remained relatively stable, but a significant reduction was observed in the reservoir water depth. In the regions where hydrological data is limited and time-series inflow statistics are not available, this approach is very useful for monitoring the hydrological conditions of the reservoir. While there are positive aspects to this work, it is also important to mention some limitations that must be addressed in future studies. Firstly, due to the lack of cloud-free images, the monsoon months were not taken in this analysis. Secondly, the satellite data used in this study has relatively coarser spatial resolution. So, future studies in this direction should use higher resolution images. Thirdly, instead of using the spectral index score as a proxy for relative water depth, calibrating water depth could enhance the scientific validity of this analysis. This research work effectively quantified the spatial and temporal reduction in hydrological consistency and water depth. However, since it relied exclusively on remote sensing data, it did not provide direct quantitative measurements of the underlying causal factors, such as sediment load or the rate of reservoir siltation. Therefore, future research should aim to integrate these observations in the inference of the drivers of hydrological degradation. Inflow and outflow monitoring would be another approach that could be incorporated into further research work and strengthen the robustness of these findings.

7 Conclusion

The present study investigated the hydrological characteristics of a Ramsar-designated wetland site through time series monitoring of satellite images. Among the three water extraction techniques employed, the Modified Normalized Difference Water Index (MNDWI) was found to be the most effective. This research analyzed dual-season monitoring of hydrological characteristics, including hydrological consistency and trends in relative water depth within the reservoir. The findings indicate that the area of consistent water cover has decreased over the past 30 years (1994-2024) during both pre- and post-monsoon seasons. Additionally, qualitative degradation in the hydrological consistency area is particularly pronounced in the fringe regions of the reservoir, highlighting an emerging threat to both ecosystem stability and ecological health. To address the challenge of limited in-situ data, this study utilized spectral water indices to estimate the relative water depth of the reservoir. It provided a comprehensive

spatio-temporal analysis of reservoir water dynamics. The results show a decreasing trend in the core area of the reservoir over time, along with a quantitatively reduced relative water depth in both the pre- and post-monsoon seasons. These trends are likely caused by a combination of factors, such as shorter wet spells and sedimentation, which are concerning indicators of habitat degradation and ecosystem loss. The findings provide the essential geospatial intelligence for developing a resilient and effective management plan that is crucial for upholding the ecological character and ensuring the long-term sustainability of the Ramsar designation. The analysis of spatial changes in hydrological consistency offers valuable insights that allow for early identification of water storage vulnerabilities. This highlights the need for proactive management strategies, such as prioritizing conservation zones and implementing adaptive water release schedules. Additionally, the use of satellite imagery is particularly effective in infrastructure-scarce conditions for measuring and monitoring reservoir water dynamics. Therefore, the study recommends applying this approach to other reservoirs to enhance water resource management and improve drought monitoring efforts.

Data availability statement

Publicly available datasets were analyzed in this study. This data can be found here: https://earthexplorer.usgs.gov.

Author contributions

RS: Methodology, Writing – original draft, Formal Analysis, Software, Data curation, Resources, Conceptualization, Writing – review and editing. PK: Methodology, Validation, Conceptualization, Supervision, Writing – review and editing, Resources.

Funding

The author(s) declare that financial support was received for the research and/or publication of this article. The first author of this research paper (RS) would like to acknowledge University Grants

References

Amasi, A., Wynants, M., Blake, W., and Mtei, K. (2021). Drivers, impacts and mitigation of increased sedimentation in the hydropower reservoirs of East Africa. *Land* 10 (6), 638. doi:10.3390/land10060638

Asher, J., Williams, I. D., and Harvey, E. S. (2017). Mesophotic depth gradients impact reef fish assemblage composition and functional group partitioning in the Main Hawaiian Islands. *Front. Mar. Sci.* 4, 98. doi:10.3389/fmars.2017.00098

Ayele, G. T., Kuriqi, A., Jemberrie, M. A., Saia, S. M., Seka, A. M., Teshale, E. Z., et al. (2021). Sediment yield and reservoir sedimentation in highly dynamic watersheds: the case of Koga Reservoir, Ethiopia. *Water* 13 (23), 3374. doi:10.3390/w13233374

Borro, M., Morandeira, N., Salvia, M., Minotti, P., Perna, P., and Kandus, P. (2014). Mapping shallow lakes in a large South American floodplain: a frequency approach on multitemporal Landsat TM/ETM data. *J. Hydrology* 512, 39–52. doi:10.1016/j.jhydrol. 2014.02.057

Cazenave, A., Champollion, N., Benveniste, J., and Chen, J. (2016). Remote sensing and water resources (Springer), 55.

Commission (UGC Ref. No.: 3430/(NET-DEC 2018)), New Delhi, India for providing financial support as a Senior Research Fellowship to conduct the research work presented in this paper. We would also like to extend our gratitude to the USGS for providing satellite images. We are also thankful to Ankur Yadav, Ashwani, and Udbhaw Sandylya for their assistance during the field survey and software handling.

Conflict of interest

The authors declare that the research was conducted in the absence of any commercial or financial relationships that could be construed as a potential conflict of interest.

Generative Al statement

The author(s) declare that no Generative AI was used in the creation of this manuscript.

Any alternative text (alt text) provided alongside figures in this article has been generated by Frontiers with the support of artificial intelligence and reasonable efforts have been made to ensure accuracy, including review by the authors wherever possible. If you identify any issues, please contact us.

Publisher's note

All claims expressed in this article are solely those of the authors and do not necessarily represent those of their affiliated organizations, or those of the publisher, the editors and the reviewers. Any product that may be evaluated in this article, or claim that may be made by its manufacturer, is not guaranteed or endorsed by the publisher.

Supplementary material

The Supplementary Material for this article can be found online at: https://www.frontiersin.org/articles/10.3389/frsen.2025.1682140/full#supplementary-material

Das, R. T., and Pal, S. (2017). Exploring geospatial changes of wetland in different hydrological paradigms using water presence frequency approach in Barind tract of West Bengal. *Spatial Inf. Res.* 25 (3), 467–479. doi:10.1007/s41324-017-0114-6

Daus, M., Koberger, K., Koca, K., Beckers, F., Encinas Fernández, J., Weisbrod, B., et al. (2021). Interdisciplinary reservoir management—a tool for sustainable water resources management. *Sustainability* 13 (8), 4498. doi:10.3390/su13084498

Debanshi, S., and Pal, S. (2020). Wetland delineation simulation and prediction in deltaic landscape. *Ecol. Indic.* 108, 105757. doi:10.1016/j.ecolind.2019.105757

Donchyts, G., Winsemius, H., Baart, F., Dahm, R., Schellekens, J., Gorelick, N., et al. (2022). High-resolution surface water dynamics in Earth's small and medium-sized reservoirs. *Sci. Rep.* 12 (1), 13776. doi:10.1038/s41598-022-17074-6

Ekka, A., Pande, S., Jiang, Y., and der Zaag, P. V. (2020). Anthropogenic modifications and river ecosystem services: a landscape perspective. *Water* 12 (10), 2706. doi:10.3390/w12102706

Feng, D. (2009). A new method for fast information extraction of water bodies using remotely sensed data. *Remote Sens. Technol. Appl.* 24 (2), 167–171. doi:10.11873/j.issn. 1004-0323.2009.2.167

- Feyisa, G. L., Meilby, H., Fensholt, R., and Proud, S. R. (2014). Automated water extraction index: a new technique for surface water mapping using landsat imagery. *Remote Sens. Environ.* 140, 23–35. doi:10.1016/j.rse.2013.08.029
- Gao, B. C. (1996). NDWI—A normalized difference water index for remote sensing of vegetation liquid water from space. *Remote Sens. Environ.* 58 (3), 257–266. doi:10.1016/s0034-4257(96)00067-3
- Garg, V., and Jothiprakash, V. (2013). Evaluation of reservoir sedimentation using data driven techniques. *Appl. Soft Comput.* 13 (8), 3567–3581. doi:10.1016/j.asoc.2013. 04 019
- Ghosh, K., and Chakraborty, P. (2021). "Assessing the benefits, threats and conservation of reservoir-based wetlands in the Eastern Himalayan River Basin," in Wetlands conservation: current challenges and future strategies, 140–161.
- Guo, Z., Boeing, W. J., Borgomeo, E., Xu, Y., and Weng, Y. (2021). Linking reservoir ecosystems research to the sustainable development goals. *Sci. Total Environ.* 781, 146769. doi:10.1016/j.scitotenv.2021.146769
- Haghighi, A. T., Marttila, H., and Kløve, B. (2014). Development of a new index to assess river regime impacts after dam construction. *Glob. Planet. Change* 122, 186–196. doi:10.1016/j.gloplacha.2014.08.019
- Ho, L. T., and Goethals, P. L. (2019). Opportunities and challenges for the sustainability of lakes and reservoirs in relation to the Sustainable Development Goals (SDGs). *Water* 11 (07), 1462. doi:10.3390/w11071462
- Kahaduwa, A., and Rajapakse, L. (2022). Review of climate change impacts on reservoir hydrology and long-term basin-wide water resources management. *Build. Res. Inf.* 50 (5), 515–526. doi:10.1080/09613218.2021.1977908
- Khatun, R., Talukdar, S., Pal, S., and Kundu, S. (2021). Measuring dam induced alteration in water richness and eco-hydrological deficit in flood plain wetland. *J. Environ. Manag.* 285, 112157. doi:10.1016/j.jenvman.2021.112157
- Krztoń, W., Walusiak, E., and Wilk-Woźniak, E. (2022). Possible consequences of climate change on global water resources stored in dam reservoirs. *Sci. Total Environ.* 830, 154646. doi:10.1016/j.scitotenv.2022.154646
- Mácová, K., and Kozáková, Z. (2023). How important for society is recreation provided by multi-purpose water reservoirs? Welfare analysis of the Vltava river reservoir system. *Water* 15 (10), 1966. doi:10.3390/w15101966
- Malik, M., and Rai, S. C. (2019). Drivers of land use/cover change and its impact on Pong Dam wetland. *Environ. Monit. Assess.* 191, 203–214. doi:10.1007/s10661-019-7347-x
- Matlhodi, B., Kenabatho, P. K., Parida, B. P., and Maphanyane, J. G. (2021). Analysis of the future land use land cover changes in the gaborone dam catchment using camarkov model: implications on water resources. *Remote Sens.* 13 (13), 2427. doi:10.3390/rs13132427
- McFeeters, S. K. (1996). The use of the normalized difference water index (NDWI) in the delineation of open water features. *Int. J. Remote Sens.* 17 (7), 1425–1432. doi:10. 1080/01431169608948714
- Monserud, R. A., and Leemans, R. (1992). Comparing global vegetation maps with the Kappa statistic. $\it Ecol.~Model.~62~(4),~275-293.~doi:10.1016/0304-3800(92)90003-w$
- Nandi, S., Patel, P., and Swain, S. (2024). IMDLIB: an open-source library for retrieval, processing and spatiotemporal exploratory assessments of gridded meteorological observation datasets over India. *Environ. Model. Softw.* 171, 105869. doi:10.1016/j.envsoft.2023.105869
- Pal, S., and Paul, S. (2021). Stability consistency and trend mapping of seasonally inundated wetlands in Moribund deltaic part of India. *Environ. Dev. Sustain.* 23, 12925–12953. doi:10.1007/s10668-020-01193-z
- Pal, S., and Sarda, R. (2021). Measuring the degree of hydrological variability of riparian wetland using hydrological attributes integration (HAI) histogram comparison approach (HCA) and range of variability approach (RVA). *Ecol. Indic.* 120, 106966. doi:10.1016/j.ecolind.2020.106966
- Pal, S., and Sarda, R. (2022). Modelling water richness in riparian flood plain wetland using bivariate statistics and machine learning algorithms and figuring out the role of damming. *Geocarto Int.* 37 (19), 5585–5608. doi:10.1080/10106049.2021.1920637
- Pal, S., Chowdhury, P., Talukdar, S., and Sarda, R. (2022). Modelling rabi crop health in flood plain region of India using time-series Landsat data. *Geocarto Int.* 37 (13), 3761–3790. doi:10.1080/10106049.2020.1869328

- Patro, E. R., De Michele, C., Granata, G., and Biagini, C. (2022). Assessment of current reservoir sedimentation rate and storage capacity loss: an Italian overview. *J. Environ. Manag.* 320, 115826. doi:10.1016/j.jenvman.2022.115826
- Paul, S., and Pal, S. (2020). Predicting wetland area and water depth of Ganges moribund deltaic parts of India. *Remote Sens. Appl. Soc. Environ.* 19, 100338. doi:10. 1016/j.rsase.2020.100338
- Połomski, M., and Wiatkowski, M. (2023). Impounding reservoirs, benefits and risks: a review of environmental and technical aspects of construction and operation. *Sustainability* 15 (22), 16020. doi:10.3390/su152216020
- Saha, T. K., Sajjad, H., Rahaman, M. H., and Sharma, Y. (2024). Exploring the impact of land use/land cover changes on the dynamics of Deepor wetland (a Ramsar site) in Assam, India using geospatial techniques and machine learning models. *Model. Earth Syst. Environ.* 10 (3), 4043–4065. doi:10.1007/s40808-024-01999-0
- Sarda, R., and Das, P. (2018). Monitoring changing trends of water presence state in the major manmade reservoirs of Mayurakshi river basin, eastern India. *Spatial Inf. Res.* 26. 437–447. doi:10.1007/s41324-018-0188-9
- Sarda, R., and Pal, S. (2024). Inundation dynamics of the natural and manmade wetlands in the Mayurakshi River basin, Eastern India. *Environ. Sci. Pollut. Res.* 31 (9), 14023–14042. doi:10.1007/s11356-024-32094-7
- Sharma, D. K., Vyas, A., Agarwal, T., and Singh, S. (2021). Challenges posed by climate change and sedimentation of reservoirs for flood mitigation and sustained water supply. *Incold J.* 10 (1), 18–30.
- Shen, L., and Li, C. (2010). "Water body extraction from Landsat ETM+ imagery using adaboost algorithm," in 2010 18th international conference on geoinformatics (IEEE), 1–4.
- Shukla, S., Jain, S. K., Kansal, M. L., and Chandniha, S. K. (2017). Assessment of sedimentation in Pong and Bhakra reservoirs in Himachal Pradesh, India, using geospatial technique. *Remote Sens. Appl. Soc. Environ.* 8, 148–156. doi:10.1016/j. rsase.2017.08.008
- Sogno, P., Klein, I., and Kuenzer, C. (2022). Remote sensing of surface water dynamics in the context of global change—a review. *Remote Sens.* 14 (10), 2475. doi:10.3390/rs14102475
- Soriano-Vargas, A., Werneck, R., Moura, R., Júnior, P. M., Prates, R., Castro, M., et al. (2021). A visual analytics approach to anomaly detection in hydrocarbon reservoir time series data. *J. Petroleum Sci. Eng.* 206, 108988. doi:10.1016/j.petrol.2021.108988
- Stevens-Rumann, C. S., Kemp, K. B., Higuera, P. E., Harvey, B. J., Rother, M. T., Donato, D. C., et al. (2018). Evidence for declining forest resilience to wildfires under climate change. *Ecol. Lett.* 21 (2), 243–252. doi:10.1111/ele.12889
- Taheri Dehkordi, A., Valadan Zoej, M. J., Ghasemi, H., Jafari, M., and Mehran, A. (2022). Monitoring long-term spatiotemporal changes in Iran surface waters using Landsat imagery. *Remote Sens.* 14 (18), 4491. doi:10.3390/rs14184491
- Talukdar, S., and Pal, S. (2019). Effects of damming on the hydrological regime of Punarbhaba river basin wetlands. *Ecol. Eng.* 135, 61–74. doi:10.1016/j.ecoleng.2019. 05.014
- Verma, S., Verma, M. K., Prasad, A. D., Mehta, D., Azamathulla, H. M., Muttil, N., et al. (2023). Simulating the hydrological processes under multiple land use/land cover and climate change scenarios in the mahanadi reservoir complex, Chhattisgarh, India. *Water* 15 (17), 3068. doi:10.3390/w15173068
- Xu, H. (2006). Modification of normalised difference water index (NDWI) to enhance open water features in remotely sensed imagery. *Int. J. Remote Sens.* 27 (14), 3025–3033. doi:10.1080/01431160600589179
- Yang, C. J., and Xu, M. (1998). Discussion on water extraction based on remote sensing information mechanism. *Geogr. Res.* 7 (Suppl. l), 86–89.
- Yang, H., Wang, J., Xiao, W., Lu, F., Wang, Y., and JarsjÖ, J. (2020). Relationship between hydroclimatic variables and reservoir wetland landscape pattern indices: a case study of the Sanmenxia Reservoir wetland on the Yellow River, China. *J. Earth Syst. Sci.* 129, 83–11. doi:10.1007/s12040-020-1347-7
- Zhai, K., Wu, X., Qin, Y., and Du, P. (2015). Comparison of surface water extraction performances of different classic water indices using OLI and TM imageries in different situations. *Geo-spatial Inf. Sci.* 18 (1), 32–42. doi:10.1080/10095020.2015.1017911
- Zhao, M., Liu, Y., Wang, Y., Chen, Y., and Ding, W. (2022). Effectiveness assessment of reservoir projects for flash flood control, water supply and irrigation in Wangmo Basin, China. *Sci. Total Environ.* 851, 157918. doi:10.1016/j.scitotenv.2022.157918